Nascent Chain Ubiquitination is Uncoupled from Degradation to Enable Protein Maturation

Xia Li[1] and Malaiyalam Mariappan[1]

Department of Cell Biology, Yale School of Medicine, Nanobiology Institute, Yale University West Campus.

[1]Department of Cell Biology
Nanobiology Institute
Yale School of Medicine
Yale West Campus
West Haven, CT 06516, USA

Correspondence: malaiyalam.mariappan@yale.edu

SUMMARY

A significant proportion of nascent proteins undergo polyubiquitination on ribosomes in mammalian cells, yet the fate of these proteins remains elusive. The ribosome-associated quality control (RQC) is a mechanism that mediates the ubiquitination of nascent chains on stalled ribosomes. In this study, we find that nascent proteins ubiquitinated on stalled ribosomes by the RQC ligase LTN1 are insufficient for proteasomal degradation. Our biochemical reconstitution studies reveal that ubiquitinated nascent chains are promptly deubiquitinated in the cytosol upon release from stalled ribosomes, as they are no longer associated with LTN1 E3 ligase for continuous ubiquitination to compete with cytosolic deubiquitinases. These deubiquitinated nascent chains can mature into stable proteins. However, if they misfold and expose a degradation signal, cytosolic quality control recognizes them for re-ubiquitination and subsequent proteasomal degradation. Thus, our findings suggest that cycles of ubiquitination and deubiquitination spare foldable nascent proteins while ensuring the degradation of terminally misfolded proteins.

INTRODUCTION

Cells face fundamental challenges in accurately selecting aberrant proteins for degradation while sparing newly synthesized proteins since both often exhibits similar biophysical characteristics such as exposed hydrophobic sequences[1]. Inefficient recognition and removal of misfolded proteins can lead to the buildup of toxic species, contributing to various neurodegenerative diseases[2,3]. Conversely, prematurely flagging newly synthesized proteins based solely on their initial biophysical properties can lead to wasted cellular energy and disruption of proteostasis. This issue is particularly pronounced during protein synthesis, as a significant portion of nascent proteins on ribosomes undergo polyubiquitination, even under unstressed conditions in both yeast and mammalian cells[4-6]. It has been debated whether all ubiquitinated nascent proteins are degraded because constant flux of ubiquitinated proteins could substantially burden the proteasome capacity and delay the degradation of toxic misfolded proteins[7-10]. Additionally, the indiscriminate degradation of nascent chains ubiquitinated on ribosomes could lead to wastage of cellular energy, given that each peptide bond formation consumes an energy equivalent of approximately ~5 ATP molecules[10,11]. Hence, gaining insight into the cellular mechanisms that distinguish terminally misfolded proteins for degradation while allowing folding-competent nascent proteins to mature holds promise in identifying therapeutic strategies for addressing human diseases linked to proteostasis breakdown.

The Ribosome-Associated Quality Control (RQC) is a mechanism responsible for ubiquitinating nascent proteins when ribosomes encounter stalls during translational elongation[12-16]. These stalls can occur under various pathological conditions, such as a deficiency in aminoacyl tRNAs or due to aberrant mRNAs[17]. Furthermore, studies have demonstrated that ribosome stalling can happen under physiological conditions. For instance, specific amino acid sequences, like arrest peptides (APs) and transmembrane domains[18-24], interact with the components in the ribosome exit tunnel components, leading to induction of ribosome stalling. These physiological stalls play a critical role in regulating processes such as protein expression, targeting, and folding[25-28]. According to the current model[13-15,29-31], RQC factors detect stalled ribosomes and facilitate their separation into 60S and 40S subunits. The E3 ligase LTN1 (Listerin)[12] is responsible for ubiquitinating nascent chains associated with the 60S subunits[32-34], a process facilitated by the protein NEMF[16,35-37]. LTN1 can also ubiquitinate ribosomes-stalled nascent chains at the Sec61 translocon of the endoplasmic reticulum (ER) [38-40]. Unlike other protein quality control systems that typically recognize substrates, LTN1 recognizes 60S ribosome subunits harboring peptidyl tRNAs bound to NEMF and mediates the ubiquitination of nascent chains regardless of their folding status[41]. The p97 ATPase is proposed to facilitate the extraction of ubiquitinated nascent chains from 60S subunits, subsequently directing them towards proteasomal degradation[16,37,42].

Despite significant progress in our understanding of the structural and mechanistic aspects of stalled ribosome recognition and nascent chain ubiquitination, the ultimate and critical stage of protein degradation remains poorly elucidated. Crucially, we understand little about the specific features that dictate the proteasomal degradation of ubiquitinated nascent chains arising from stalled ribosomes. Pioneering studies employing model substrates with aberrant mRNAs, which induce ribosome stalling, played a pivotal role in the identification and characterization of RQC factors[13-15,29,30,43]. However, these mRNAs often lead to the production of aberrant proteins, which prompts questions about the mechanisms of nascent chain degradation. Consequently, it remains unclear whether these faulty proteins are also targeted by cytosolic quality control for ubiquitination and subsequent proteasomal degradation.

To address these fundamental questions, we investigated the endogenous stalling substrate XBP1u, a pivotal player in the unfolded protein response (UPR)[44,45]. This substrate encompasses a small hydrophobic region 1 (HR1), a long HR2, and a translational arrest peptide (AP) at the C-terminus[26,46]. XBP1u AP makes extensive contacts with the ribosomal exit tunnel components and forms a unique turn in proximity to the peptidyl transferase center, ultimately leading to translational arrest[47]. We and others have previously shown that the translationally arrested XBP1u mRNA ribosome-nascent chains (RNCs) expose a hydrophobic region 2 (HR2) for the recognition by the signal

recognition particle (SRP) and targeting to the Sec61 translocon at the ER membrane [48,49]. In our investigation of XBP1u, we discovered that ubiquitinated nascent chains, catalyzed by LTN1 on stalled ribosomes, undergo rapid deubiquitination by cytosolic deubiquitinases upon their release. Their proteasomal degradation relies entirely on whether the nascent chain exposes a degradation signal in the cytosol for subsequent re-ubiquitination. Hence, our results indicate that the separation of ubiquitination of nascent chains on ribosomes from immediate proteasomal degradation offers a chance for the maturation of folding-competent proteins, while also preventing premature degradation, thus conserving energy expended on protein synthesis.

RESULTS

Nascent chains stalled on ribosomes are ubiquitinated by LTN1 E3 ligase

To determine the fate of ubiquitinated nascent chains on ribosomes, we investigated the degradation of XBP1u, which induces ribosomal stalling during translation elongation[26] (Figure 1A). Recent ribosome profiling studies have proposed that the degradation of XBP1u nascent chains is facilitated by the RQC pathway[21]. Nonetheless, it remains unclear whether the RQC E3 ligase, LTN1, is responsible for ubiquitinating XBP1u on ribosomes and if this ubiquitin modification mediates proteasomal degradation. To address these questions, we initially investigated whether the translationally paused XBP1u-ribosome nascent chains (RNCs) recruit the LTN1 E3 ligase and its cofactor NEMF[16,35-37]. Immunoblotting of sucrose density gradient fractions from wild type (WT) 293T cells revealed that both LTN1 and NEMF1 primarily co-fractionated in the non-ribosomal top fractions, with only a minor fraction localized to the ribosomal fractions (8 to 10) (Figure 1B). In cells expressing XBP1u, as expected, translationally stalled XBP1u co-migrated with ribosomes. Additionally, a notable portion of LTN1, along with nearly the entire population of NEMF, shifted to ribosomal fractions, indicating that XBP1u-induced ribosome stalling initiates the recruitment of these factors. Consistent with earlier studies, the binding of NEMF to ribosomes appeared independent of LTN1, as its entire population was recruited to stalled XBP1u ribosomes in LTN1 knock-out (KO) cells generated by CRISPR/Cas9. Immunoprecipitation experiments further confirmed the association of XBP1u RNCs with LTN1 and NEMF (Figure 1C).

To asses if LTN1 E3 ligase activity is required for proteasomal degradation of XBP1u, we examined the stability of endogenous XBP1u in both WT and LTN1 KO cells. Due to its inherently unstable nature, endogenous XBP1u was not readily detectable in WT cells(Figure 1D). However, inhibition of the proteasome with MG132 led to an accumulation of XBP1u protein, indicating that XBP1u is subjected to degradation by proteasomes. Remarkably, levels of XBP1u protein were significantly elevated in LTN1-depleted cells, even in the absence of MG132 treatment (Figure 1D). Transient expression of recombinant XBP1u exhibited similar behavior to its endogenous counterpart,

accumulating in LKO or LTN1-depleted cells using siRNA when compared to control cells (Figure S1A, S1B). This accumulation of XBP1u was restorable through the complementation of WT LTN1, but not with LTN1 lacking the catalytic RING domain (LTN1ΔRING), suggesting that LTN1-mediated ubiquitination plays a crucial role in regulating XBP1u protein levels in cells (Figure S1C). Both pulse chase and cycloheximide chase experiments further illustrated that XBP1u underwent rapid turnover in WT cells, while degradation was impeded in LKO cells (Figure 1E and S1D). In contrast, the ribosomal arrest mutant XBP1u-AP* was subject to degradation in an LTN1-independent manner, as it exhibited a similar turnover rate in both WT and LKO cells (Figure 1F and S1E).

To further elucidate whether LTN1 mediates XBP1u ubiquitination, we co-expressed XBP1u along with HA-ubiquitin in both WT and LKO cells. Subsequently, XBP1u was immunoprecipitated using anti-FLAG antibodies, followed by probing for ubiquitin-conjugated XBP1u via immunoblotting. The ubiquitinated species, characterized by ladder and/or smear bands, were readily discernible in WT cells, while their presence in LKO cells was nearly diminished (Figure 1G). Similarly, XBP1u-AP* exhibited ubiquitination but independent of LTN1 activity (Figure 1H), aligning with its degradation observed in both WT and LKO cells (Figure 1F and S1E). When probed with a K48-linked ubiquitin chain specific antibody, it became evident that the polyubiquitinated species of both XBP1u and XBP1u-AP* were enriched in K48-linked ubiquitin chains, which are known to be optimal for directing proteins for proteasomal degradation (Figure 1I). Together, these data suggest that XBP1u represents a unique substrate, being ubiquitinated and subsequently degraded irrespective of ribosome stalling.

LTN1-mediated ubiquitination is dispensable for the degradation of stalled nascent chain

The ubiquitination and subsequent degradation of XBP1u-AP* indicate that XBP1u contains a degron mediating proteasomal degradation. Given that XBP1u contains a long hydrophobic sequence (HR2) and is exposed to the cytosol due to its inability to insert into the ER membrane, we tested the role of HR2 in mediating the degradation of XBP1u. To this end, we generated XBP1u with HR2 deleted (ΔHR2) and mutated HR2 to increase its hydrophobicity by replacing less hydrophobic amino acids with hydrophobic leucines (4L) (Figure 2A). We hypothesized that ΔHR2 would display increased stability due to the absence of hydrophobicity, while 4L should remain stable owing to its proper insertion into the ER membrane.

In support of our hypothesis, the deletion of HR2 resulted in the stabilization of XBP1u in both WT and LKO cells, as demonstrated by pulse-chase experiments using radiolabeling and cycloheximide (CHX) chase assays (Figure 2B and S2A). The reduced degradation of ΔHR2 was not attributable to a lack of ubiquitination, as it was ubiquitinated in an LTN1-dependent manner (Figure 2C). Similar LTN1-dependent ubiquitination was observed when HR2 was replaced with a hydrophilic

sequence, thus excluding the potential effects caused by HR2 deletion (Figure S2B). Interestingly, strengthening the hydrophobicity of XBP1u (4L) resulted in the inhibition of XBP1u degradation in WT cells (Figure 2D), despite being ubiquitinated in an LTN1-dependent manner (Figure 2E). This is because 4L is known to be efficiently inserted into the ER membrane, thereby preventing exposure to the cytosolic quality control[50]. Collectively, these data suggest that exposed hydrophobicity plays a critical role in the degradation of nascent chains, but not in AP-dependent ubiquitination that initially occurs on ribosomes (Figure 2F).

Nascent chains ubiquitinated by LTN1 are deubiquitinated in the cytosol

The above data suggest a model where XBP1u undergoes two rounds of ubiquitination: first by LTN1 on stalled ribosomes, and second through HR2-dependent ubiquitination in the cytosol. To investigate this, we separated ribosomes from supernatants using a sucrose cushion and probed for ubiquitin-conjugated XBP1u (Figure 3A). Since the nascent chain remains attached to ribosomes, it would co-sediment with them, whereas released nascent chains would be found in the supernatant. This allowed us to distinguish AP-dependent nascent chain ubiquitination on ribosomes from HR2-dependent ubiquitination in the cytosol. Consistent with our model, ubiquitinated XBP1u was detectable in both ribosome and supernatant fractions in WT cells (Figure 3B). However, the depletion of LTN1 in LKO cells primarily reduced the ubiquitin signal in the ribosome fraction, supporting the idea that cytosolic ubiquitination of XBP1u is independent of LTN1 activity. Probing with a K48-linked ubiquitin chain specific antibody revealed that nascent chains on ribosomes were modified with K48-linked ubiquitin chains by LTN1 (Figure S3A). Complementation experiment confirmed that the catalytic RING domain of LTN1 is essential for the ubiquitination of XBP1u nascent chains on stalled ribosomes (Figure S3B). In contrast to XBP1u, we observed only monoubiquitinated ΔHR2 in the cytosol fractions of both WT and LKO cells (Figure 3C). Conversely, the ubiquitination of ΔHR2 in the ribosome fraction strictly depended on LTN1 activity. As anticipated, the stalling mutant XBP1u-AP* was exclusively ubiquitinated in the supernatant, and this ubiquitination was consistent in both WT and LKO cells (Figure 3D).

To further support the aforementioned observation that XBP1u undergoes two rounds of ubiquitination, we fractionated cell lysates of both XBP1u and ΔHR2 on a sucrose density gradient. Immunoprecipitation for XBP1u was performed on all fractions, followed by probing for ubiquitinated proteins. Immunoblotting for ribosomal protein RPL9 indicated that the majority of ribosomes localized in fractions 6 to 8 (Figure 3E). XBP1u exhibited both AP and HR2-dependent ubiquitination, as evidenced by the presence of ubiquitinated bands in both the peak ribosomal fractions (6-8) and the non-ribosomal fractions (1-3) (Figure 3E). In sharp contrast, ΔHR2 displayed AP-dependent

ubiquitination in the ribosomal fractions but largely lacked HR2-dependent ubiquitin modifications in the non-ribosomal fractions (Figure 3F). AP-dependent ubiquitination for both XBP1u and ΔHR2 observed in the ribosomal fractions was diminished in LKO cells, further confirming that LTN1 is responsible for ubiquitination of nascent chains on stalled ribosomes (Figure S3C and S3D). These results lead to the hypothesis that AP-dependent ubiquitin modifications are removed from nascent chains. To test this hypothesis, we monitored the status of ubiquitin modifications on XBP1u after inhibiting protein synthesis with cycloheximide (CHX). Both ubiquitin and total protein signals diminished during the CHX chase, indicating that ubiquitinated XBP1u is rapidly degraded (Figure 3G). In contrast, ubiquitin chains of ΔHR2, which occurred only on ribosomes (Figure 3F), were swiftly removed with little change in the ΔHR2 protein level during a 3-hour chase (Figure 3G), indicating that AP-dependent ubiquitin chains undergo deubiquitination. The disappearance of ubiquitin signals for XBP1-AP* along with a concomitant loss of total proteins (Figure 3G) supports the notion that HR2-dependent ubiquitination is sufficient for proteasomal degradation.

Dissociation of nascent chains from stalled ribosomes results in deubiquitination and re-ubiquitination in the cytosol

To elucidate the mechanism of XBP1u nascent chain deubiquitination, we reconstituted ubiquitination and deubiquitination reactions in vitro. We generated XBP1u or ΔHR2 ribosome-associated nascent chains (RNCs) by translating transcripts lacking a stop codon in the rabbit reticulocyte lysate (RRL)-based translation system, including His-ubiquitin and radiolabeled 35S-methionine. The translationally stalled RNCs were ubiquitinated in the RRL, as evidenced by talon pull-down, which enriched for His-tagged ubiquitin-conjugated XBP1u or ΔHR2 (Figure 4A). Furthermore, ubiquitination of RNCs was notably enhanced when incubated with cytosol prepared from WT HeLa cells. In contrast, incubation with cytosol derived from LTN1 KO cells did not significantly increase ubiquitination (Figure 4A). This result confirms that LTN1 E3 ligase mediates the ubiquitination of nascent chains on stalled ribosomes. Notably, the level of ΔHR2 ubiquitination was comparable to WT XBP1u, indicating that LTN1 mediates the ubiquitination of nascent chains on stalled ribosomes regardless of whether they contain exposed hydrophobicity (HR2). To determine if nascent chain dissociation from ribosomes alone is sufficient for deubiquitination, we treated RNCs with puromycin in the presence of cytosol. Puromycin mimics aminoacyl tRNA and releases nascent chains as peptidyl-puromycin derivatives[51]. Puromycin treatment of XBP1u RNCs resulted in the loss of polyubiquitinated species and the detection of lower ubiquitinated species (Figure 4B). These bands did not appear when an E1 inhibitor (MLN7243)[52], which inhibits re-ubiquitination, was included during the puromycin treatment. This suggests that they represent re-ubiquitination of XBP1u in the cytosol rather than leftover ubiquitins from deubiquitination.

In contrast, the ubiquitin chains of ΔHR2 were nearly entirely lost upon puromycin treatment, with little re-ubiquitination occurring (Figure 4B). Fractionation after puromycin treatment further revealed that re-ubiquitinated XBP1u and deubiquitinated ΔHR2 were localized to the supernatant cytosol fractions (Figure 4C).

Next, we monitored the dynamics of deubiquitination and re-ubiquitination by treating RNCs with puromycin in the presence of cytosol and sampled at various time points to assess ubiquitin-conjugated proteins. Figure 4D shows that polyubiquitinated species mostly disappeared within 5 minutes of nascent chain release by puromycin. Remarkably, newly ubiquitinated XBP1u began to emerge after 30 minutes, indicating re-ubiquitination in the cytosol. The re-ubiquitination of XBP1u could be entirely inhibited when the E1 inhibitor was included along with puromycin, providing support for the involvement of a cytosolic E3 ligase(s) in mediating the re-ubiquitination of XBP1u. In contrast to XBP1u, ubiquitin chains on ΔHR2 were largely removed within 30 minutes with no new ubiquitin modifications occurring, and little change was observed when including the E1 inhibitor (Figure 4E). This result implies that the exposed hydrophobicity of HR2 in XBP1u is strictly required for re-ubiquitination in the cytosol.

Cytosolic deubiquitinases (DUBs) were responsible for removing ubiquitin chains from nascent chains, as evidenced by the reduced deubiquitination of nascent chains when the cytosol was treated with the generic DUB inhibitor PR-619[53] (Figure 4F). These findings suggest that the dissociation of nascent chains from the ribosome-LTN1 E3 ligase complex is sufficient for their deubiquitination by cytosolic DUBs. Additionally, our results propose a paradigm whereby substrates undergo continuous modifications by their respective E3 ligases to effectively compete against cytosolic DUBs. To explore this, we generated polyubiquitinated XBP1u or ΔHR2 RNCs and incubated them with untreated or E1 inhibitor-treated cytosol. Strikingly, ubiquitin chains on nascent chains were mostly removed in the presence of E1 inhibitor-treated cytosol, even though they remained attached to stalled ribosomes (Figure S5A). This observation is not exclusive to LTN1-mediated ubiquitination occurring on stalled ribosomes, as the stalling mutant XBP1u-AP*, ubiquitinated by the cytosolic quality control, also underwent deubiquitination when incubated with the E1 inhibitor (Figure S5B). These data suggest that cytosolic DUBs constantly remove ubiquitin chains from nascent chains, providing an opportunity for protein maturation. However, if a deubiquitinated protein consistently exposes a hydrophobic region, as observed with XBP1u, it is then recognized by the cytosolic quality control for re-ubiquitination.

Protein folding status determines re-ubiquitination and degradation of nascent proteins

To further substantiate our model, which posits that cytosolic quality control, rather than the RQC, governs the degradation of nascent chains, we sought to identify the quality control machinery

responsible for recognizing the exposed hydrophobicity (HR2) in XBP1u in the cytosol. Given the known role of the Bag6 complex in recognizing long hydrophobic sequences in proteins and mediating ubiquitination, we performed a co-immunoprecipitation to probe the interaction between XBP1u and Bag6[24,54]. Bag6 interreacted with XBP1u and XBP1u-AP*, both of which contain HR2, and weakly interacted with ΔHR2, as expected (Figure 5A). Notably, XBP1u interaction with Bag6 was further intensified when proteasomes were inhibited with MG132, indicating that Bag6-associated XBP1u is routed for proteasomal degradation. To determine if the Bag6-associated E3 ligase RNF126[55] is responsible for mediating the ubiquitination of XBP1u in cells, we depleted RNF126 using siRNA oligos and monitored the ubiquitination of both XBP1u and XBP1u-AP*. Indeed, the ubiquitination of both XBP1u and XBP1u-AP* was significantly reduced in RNF126-depleted cells compared to control siRNA-treated cells (Figure 5B). Pulse-chase and cycloheximide chase experiments further confirmed that the degradation of both XBP1u and XBP1u-AP* relied on RNF126 E3 ligase activity, as evidenced by their impaired degradation in RNF126-depleted cells relative to control knockdown cells (Figure 5C and Figure S5A and S5B).

Our data so far strongly indicate that the initial ubiquitination occurring on ribosomes does not dictate the fate of the nascent chain. Instead, it is the exposed hydrophobicity, a characteristic often exhibited by misfolded proteins, that plays a pivotal role in driving re-ubiquitination in the cytosol, ultimately leading to proteasomal degradation. To directly scrutinize this model, we capitalized on an engineered destabilized domain (dd) containing FKBP12, which can be stabilized by incubation with a folding-stabilizing ligand, Shield1 (Figure 5D)[56]. We predict that if nascent chain ubiquitination occurring on stalled ribosomes is sufficient for proteasomal degradation, we would expect to observe the degradation of ddFKBP12 even in the presence of Shield1. To this end, the C-terminus of ddFKBP12 was appended with the AP sequence from XBP1u. ddFKBP-AP underwent ubiquitination in an LTN1-dependent manner, both in the presence and absence of the folding stabilizer Shield1 (Figure 5E). As expected, ddFKBP-AP was subject to degradation in the absence of Shield1 due to its misfolding (Figure 5F and Figure S5C). Surprisingly, ddFKBP-AP exhibited significant stabilization in the presence of Shield1, despite being ubiquitinated by LTN1. We obtained similar results when ddFKBP was fused with a stronger AP sequence, which known to induce stronger translational pausing[26] (Figure S5C and Figure S5D). These results provide further support for the model that ubiquitinated nascent chains on stalled ribosomes have the capacity to undergo deubiquitination and subsequently fold into native proteins.

LTN1-mediated release of nascent chains from stalled ribosomes is critical for eliciting proper UPR

Given that LTN1-mediated ubiquitination is found to be dispensable for proteasomal degradation, we asked what is the purpose of LTN1-mediated ubiquitination? We hypothesized that the activity of the LTN1 E3 ligase may be strictly necessary for releasing nascent chains from stalled ribosomes, enabling them to either undergo degradation or mature based on their biophysical characteristics. To explore this hypothesis, we initially examined the localization of endogenous XBP1u in LTN1 KO cells. Fractionation experiments revealed a predominant accumulation of endogenous XBP1u with ribosomes in LTN1 KO cells in comparison to WT cells (Figure 6A). The release of XBP1u from stalled ribosomes is dependent on the ligase activity of LTN1. This is supported by the complementation of the LTN1 RING domain mutant (ΔRING), which exhibited a similar XBP1u accumulation as observed in LTN1 KO cells. In contrast, complementation with WT LTN1 restored the release of XBP1u from ribosomes (Figure 6B). We further investigated the LTN1-dependent release of XBP1u from stalled ribosomes by conducting localization studies in 293T cells. Immunofluorescence staining demonstrated that XBP1u primarily exhibits an ER-like pattern in both WT and LTN1 KO cells (Figure 6C and 6D). While only a small fraction of XBP1u was localized to the nucleus in non-treated cells, a brief inhibition of proteasomes with MG132 resulted in a significant accumulation of XBP1u in the nucleus of WT cells due to its nuclear localization signal[57]. In contrast, the localization pattern of XBP1u did not noticeably change upon MG132 treatment of LTN1 KO cells, as it remained confined to the ER (Figure 6C and 6D), supporting the LTN1-mediates the release of XBP1u nascent chains from the ER membrane. XBP1u was associated with the ER membrane as RNCs since it could be readily released by treating cells with puromycin prior to immunostaining (Figure S6). Furthermore, neutral page (NUPAGE)-based immunoblotting, which preserves the ester bonds between tRNAs and nascent chains during SDS-PAGE electrophoresis, revealed a notable accumulation of tRNA attached XBP1u nascent chains in LTN1 KO cells relative to WT cells. As anticipated, XBP1u-AP* showed a loss of tRNA-linked XBP1u, while S255A showed increased levels of tRNA-linked XBP1u in WT cells, with further accumulation in LTN1 KO cells (Figure 6E).

Given the profound accumulation of XBP1u RNCs in the ER membrane of LTN1 KO cells, we wondered whether this would impact IRE1α-mediated XBP1u splicing during ER stress. Remarkably, the production of both spliced and unspliced forms of XBP1 was significantly increased in LTN1 KO cells treated with the ER stress inducer tunicamycin compared to WT cells (Figure 6F). Additionally, IRE1α exhibited hyperactivation and displayed a delay in inactivation during prolonged ER stress, as evidenced by the phosphorylation status of IRE1α probed by Phos-tag based immunoblotting (Figure 6F). Notably, the depletion of LTN1 selectively dysregulated the IRE1α branch of the UPR, since the activation and inactivation of the ATF6α and PERK branches behaved similarly in both WT and LTN1 KO cells. This is consistent with our earlier findings that only the IRE1α branch is associated with the

Sec61 translocon complex[48,58], where XBP1u RNCs are recruited. Collectively, our data suggest that the central role of LTN1-mediated ubiquitination is to facilitate the release of nascent chains from stalled ribosomes, thereby contributing to the maintenance of protein homeostasis.

DISCUSSION

About 5% to 15% of nascent proteins undergo ubiquitination while on ribosomes[4,5], but the mechanisms and features in these proteins that mediate proteasomal degradation has remained unclear. In this study, we systematically unraveled the degradation mechanisms of nascent chains ubiquitinated on ribosomes using a physiologically crucial protein, XBP1u, which induces ribosomal stalling through its C-terminal arrest peptide (AP) during translation elongation[26]. Our investigations revealed a robust ubiquitination of the XBP1u nascent chain on stalled ribosomes by LTN1 E3 ligase. Strikingly, despite possessing K48-linked ubiquitin chains, which are typically associated with proteasomal degradation[59], ubiquitin chains on nascent chains are promptly removed by cytosolic deubiquitinases upon their release from stalled ribosomes. Our data from in vitro experiments suggest that once the ubiquitinated nascent chain is liberated from the LTN1 E3 ligase-ribosome complex, it can no longer receive new ubiquitin modifications to effectively compete against cytosolic deubiquitinases, resulting in complete deubiquitination. By studying XBP1u mutants, we further found that deubiquitinated nascent proteins can attain stability (Figure 7). However, if they persistently expose a hydrophobic sequence, they become targets for recognition by the cytosolic quality control machinery. This leads to re-ubiquitination and subsequent proteasomal degradation.

The data presented here highlight that the nascent chain's biophysical properties, particularly its folding status as supported by the results using a conditionally folded FKBP12 mutant (Figure 5E, 5F), play a crucial role in determining whether it engages with the cytosolic quality control for degradation or achieves stability. This is in contrast to the initial ubiquitination event occurring on ribosomes, which does not seem to be the primary determinant of the nascent chain's fate. The mechanism revealed in our studies acts as a safeguard, potentially preventing the indiscriminate degradation of numerous proteins known to induce ribosomal stalling through their C-terminal sequences[20,21]. This allows these proteins to potentially fold into functional forms in the cytosol after release from stalled ribosomes.

Our findings may also shed light on why cells have evolved an alternative but conserved mechanism to add C-terminal Ala tails in mammals[60] (or in yeast, C-terminal Ala and Thr tracts known as CAT tails)[36,61] in an mRNA-independent but NEMF-assisted manner. This C-terminal tail ensures the recruitment of the cytosolic quality control for ubiquitination and subsequent degradation of stalled nascent proteins[60,62]. It appears unlikely that XBP1u undergoes NEMF-mediated mRNA-independent

C-terminal alanine tailing. This is because the translational elongation facilitated by NEMF may not be able to advance the XBP1u AP, which interacts with components of the ribosome exit tunnel[47]. It is tempting to speculate that commonly used model RQC substrates, which contain C-terminal poly lysines, may themselves be recognized by a cytosolic quality E3 ligase for a second round of ubiquitination and subsequent proteasomal degradation. This would explain the discrepancy between our results, which show complete stabilization of ddFKBP12-AP in the presence of the fold stabilizer Shield 1, and earlier reports demonstrating the degradation of ddFKBP12 fused with a poly(A) tail (encoding poly lysines)[41]. By contrast, the AP of XBP1u does not have any obvious degron motif for recognition by cytosolic quality control.

While our results indicate that LTN1-mediated ubiquitin chains on nascent chains may not be essential for directing them towards proteasomal degradation, our results clearly demonstrate that the activity of the LTN1 E3 ligase is crucial for the efficient release of XBP1u nascent chains from stalled ribosomes (Figure 6). Failure to release XBP1u RNCs from the ER membrane in LTN1 KO cells leads to heightened activation of IRE1α and elevated levels of spliced XBP1 factor during ER stress. Further studies are warranted to precisely elucidate how LTN1-mediated ubiquitination facilitates the release of nascent chains from stalled ribosomes bound to the Sec61 translocon. Additionally, it will be important to understand the coordination between LTN1-mediated release of XBP1u and IRE1α-mediated splicing of XBP1u during ER stress. However, LTN1-mediated ubiquitination may be dispensable for substrates that do not induce ribosome stalling through interaction with the ribosome exit tunnel. In such cases, nascent chains are released through the action of the endonuclease ANKZF1, which severs tRNAs from nascent chains on 60S ribosomal subunits[63-65] .

Two particularly intriguing observations emerged from our biochemical reconstitution experiments. Firstly, we noted that ubiquitinated nascent chains are swiftly deubiquitinated upon their release from ribosomes, but intriguingly, re-ubiquitination only becomes apparent after approximately 30 minutes (Figure 4D). This observation suggests that the initial ubiquitin modifications occurring on ribosomes may prevent an immediate recognition by the cytosolic quality control machinery. This, in turn, could provide an opportunity for protein maturation following deubiquitination, as exposed hydrophobic sequences find their place within the folded proteins. The second notable observation pertains to the complete deubiquitination of XBP1u following a brief treatment with an E1 inhibitor (Figure S4). This suggests that substrates must undergo continuous ubiquitination to effectively compete with cytosolic DUBs, which is consistent with the earlier observation that cytosolic DUBs can efficiently trim ubiquitin chains from the substrate that interacts weakly with an E3 ligase [66]. Our results also imply that a substrate should consistently present a degron, allowing it to engage with an E3 ligase complex for efficient ubiquitination and subsequent degradation by proteasomes.

Our findings suggest that the re-ubiquitination of stalled nascent chains in the cytosol is an essential step for their subsequent proteasomal degradation (Figure 7). Yet, it remains a critical area of investigation whether these nascent chains, ubiquitinated for the second time in the cytosol, are directly shuttled for proteasomal degradation. Alternatively, it is plausible that these proteins undergo cycles deubiquitination and re-ubiquitination before ultimately reaching the degradation stage. This mechanism is similar to how N-glycans play a crucial role in overseeing the folding and quality control of nascent glycoproteins[67]. This cycle of ubiquitination and deubiquitination may explain why proteasomal degradation of a substrate is very slow and often take hours in cells, which is in contrast to the relatively rapid ubiquitination and proteasomal degradation that can occur within minutes for proteins of average size[68,69].

We propose that the mechanism elucidated here may extend to retrotranslocated proteins from the ER associated protein degradation (ERAD) pathway[70]. Once these ubiquitinated proteins are extracted into the cytosol, they likely undergo deubiquitination due to their dissociation from the ER membrane-bound E3 ligase. This hypothesis may provide an explanation for the requirement of factors like Bag6[71] and other cytosolic quality control components[72] in the process of re-reubiquitination and subsequent proteasomal degradation. Furthermore, it is plausible that, similar to deubiquitinated nascent chains attaining stability, certain retrotranslocated proteins such as cholera toxin[73] and viral proteins[74] could potentially achieve their mature conformation within the cytosol.

In summary, our studies suggest that cells have uncoupled ubiquitination from proteasomal degradation to provide chances for maturation of folding-competent proteins while ensuring the degradation of terminally misfolded proteins that consistently expose a degron. However, this mechanism poses a risk for accumulating aberrant nascent proteins that cannot display any degron signatures. For instance, deubiquitination of disease-causing proteins like huntingtin (mHTT), which is known to induce ribosome stalling during translation[75,76], could delay proteasomal degradation and promote aggregation of mHTT in the cytosol. Moreover, during proteotoxic stress conditions such as aging, re-ubiquitination of stalled aberrant nascent proteins may be inefficient in the cytosol, potentially leading to the accumulation of toxic proteins in cells. Hence, targeting cytosolic DUBs responsible for deubiquitinating nascent chains could hold therapeutic potential for promoting the degradation of mHTT and other stalled aberrant nascent proteins, which are particularly exacerbated during aging[23].

ACKNOWLEDGEMENTS

We would like to thank the former and present members of the Mariappan lab for valuable discussions. Special thanks to Susan Shao (Harvard Medical School) for generously providing the LTN1 and LTN1 (ΔRING) plasmids, and to Zairong Zhang for the ddFKBP12 plasmid. This work was supported by NIH

grants R01GM117386 (M.M) and a pilot award from the Yale Diabetes Research Center (P30 DK045735).

AUTHOR CONTRIBUTIONS

XL designed and conducted all experiments. MM conceived and oversaw the project. MM drafted the manuscript with contributions from XL.

DECLARATION OF INTERESTS

The authors declare no competing interests.

METHOD DETAILS

DNA constructs, siRNAs, and antibodies

The mammalian cell expression vector pcDNA5/FRT/TO (Invitrogen, Carlsbad, CA) containing FLAG-tagged XBP1u, XBP1uΔHR2, XBP1u-AP* (L246A and W256AW), or XBP1u (S255A) was previously detailed[48]. XBP1u 4L was created by introducing Q197L, Q198L, S200L, and S203L mutations using a site-directed mutagenesis protocol. Mammalian expression constructs of FLAG-LTN1 and FLAG-LTN1ΔRING were generously provided by Dr. Susan Shao (Harvard Medical School). The XBP1u arrest peptide (AP) sequence of 26 amino acids was fused to the C-terminus of the destabilizing mutant of FKBP12 L106P (kindly provided by Dr. Zairong Zhang, University of Chinese Academy of Sciences) using a standard cloning procedure. All PCR reactions were performed with Phusion high-fidelity DNA polymerase (New England Biolabs, Ipswich, MA), except for site-directed mutagenesis, which used Pfu-Ultra polymerase (Agilent Technologies, Santa Clara, CA). 3% DMSO was included in all PCR reactions to enhance amplification. The coding regions of all constructs were sequenced to prevent any sequence errors. LTN1 siRNA (CAAACUUCCUGCAAGAUUA) and RNF126 siRNA (CGGAUUAUAUCUGUCCAAG) were synthesized from Sigma-Aldrich. Antibodies used for immunoblotting are as follows: Rabbit α-LTN1 (Proteintech; #28452-1-AP); Rabbit α-NEMF (Bethyl; # A305-758A), rat α-FLAG L5 (BioLegend; #12775); mouse α-HA-HRP (Cell Signaling Technology; #2999S); mouse α-tubulin (Abcam; #ab7291); goat α-rat-HRP (Cell Signaling Technology; #7077), goat α-mouse-HRP (Jackson ImmunoResearch; #115-035-003); goat α-rabbit-HRP (Jackson ImmunoResearch; #111-035-003); goat α-rat IgG-Cy2 (Jackson ImmunoResearch; #112–225-167); Rabbit α-XBP1u (Cell signaling Technology; # #12782). PERK, IRE1α, and ATF6α have been previously described [77]. Rabbit α-FLAG, and rabbit α-Bag6 are a gift from Dr. Ramanujan Hegde (MRC Laboratory of Molecular Biology, Cambridge, UK).

Cell culture and generation of CRISPR/Cas9-mediated knockout cell lines

HEK293T and HeLa cells were cultured in high-glucose DMEM (Corning) supplemented with 10% FBS (Gibco), 100 U/ml penicillin, and 100 mg/ml streptomycin (Gibco) at 37°C with 5% CO2. Regular mycoplasma testing was performed using the MycoStrip kit from Invivogen. Knockout cell lines were generated using the CRISPR/Cas9 system as previously described[78,79]. Cells were transfected with pSpCas9(BB)-2A-Puro (Addgene; #62988) and gRNA expression plasmid targeting LTN1. Two targeting sequences were used: 5′-AATGCCGAACGACAGTGAA-3′ and CGTGTACTTGGTAATACGT. gRNAs were designed using the web tool CHOPCHOP (version 3)[80]. Transfected cells were grown for 24 hours and then treated with 4μg/ml puromycin for 3 to 4 days until all control cells had died. Most experiments were conducted using mixed knockout clones of LTN1, as these exhibited over 90% depletion of LTN1, as confirmed by immunoblotting. In some cases, single-cell clones were isolated by plating at a density of 0.5 cells/well in 96-well plates. All knockouts were confirmed by immunoblotting.

Metabolic labeling and immunoprecipitation

HEK293T cells (0.35 × 10^6/well) were seeded onto polylysine-coated plates (0.15 mg/ml) in 12-well format and transiently transfected with 0.8 μg of the specified plasmids using 2 μl of Lipofectamine 2000 (Invitrogen). For metabolic labeling, cells were washed once with 1× PBS and then incubated in cysteine- and methionine-free media supplemented with 5% dialyzed FBS for 45 minutes. Subsequently, cells were labeled with 80 μCi/ml of Express ^{35}S Protein Labeling Mix (PerkinElmer; #NEG072014MC) for 30 minutes. The cells were then rinsed with 1× PBS and chased with complete DMEM medium containing 2 mM methionine and 2 mM cysteine. The labeled cells were directly lysed in 0.5 ml RIPA buffer and centrifuged for 15 minutes at 20,000xg. The resulting supernatant was subjected to immunoprecipitation using Rat anti-FLAG beads (BioLegend). The immunoprecipitants were subsequently analyzed by SDS-PAGE followed by autoradiography

Cycloheximide chase

HEK293T (0.125 × 10^6/well) were plated on a polylysine pre-coated 24-well–plate and transiently transfected with 0.4 μg of the indicated construct as described in the figure legends. After 24h of transfection, cells were treated with cycloheximide (100 μg/ml). The treated cells were directly harvested with 150 μl of 2× SDS sample buffer at the indicated time points. In some cases, cells were treated with both cycloheximide and MG132 (20 μm). Samples were then analyzed by immunoblotting with the indicated antibodies as described in the figure legends.

Immunoprecipitation of ubiquitinated proteins from cells

To examine total ubiquitination of XBP1u and its mutants, HEK293 cells (0.35 × 10^6/well) were seeded on polylysine-coated six-well plates and transiently transfected with 0.6 µg of XBP1u and 0.4 µg of HA-Ubiquitin using 2 µl of Lipofectamine-2000. After 24 hours of transfection, cells were washed once with 1xPBS and directly harvested using 120 µl of Tris/SDS buffer (1% SDS/100mM Tris-HCl pH 8.0). The samples were boiled for 10 minutes and a 15 µl aliquot was directly analyzed by immunoblotting as input. The remaining samples were diluted with 1 ml of Triton buffer (50mM Tris-HCl pH 8.0, 150mM NaCl, 1% Triton X-100) and immunoprecipitated using anti-FLAG beads, followed by immunoblotting analysis.

Sucrose density gradient analysis

For the sucrose gradient analysis presented in Figure 1B, HEK293T cells (1.5 × 10^6/well) were seeded onto polylysine-coated 60 cm dishes and transiently transfected with 4µg of the specified plasmids using 16 µl of PEI (1mg/ml). After 24 hours of transfection, cells were harvested in 1x PBS. The cell pellet was resuspended in 250 µl of lysis buffer (50mM Hepes, pH 7.4, 100mM KAc, 5mM MgCl2, 1% Triton X-100, 2.5u/ml of RNasin (Promega), and EDTA-free protease inhibitor (PI) from Roche) and incubated for 15 minutes on ice. Cell lysates were centrifuged at 20,000xg for 5 minutes. The resulting supernatant (200 µl) was carefully applied onto a 10% to 30% sucrose gradient and centrifuged for 80 minutes at 215,000xg using a TLS-55 rotor at 4°C with the slowest acceleration and deceleration settings. After the centrifugation, 12 x 165 µl fractions were collected and subsequently analyzed by immunoblotting.

For the sucrose gradient data presented in Figure 3E, 3F, S3B, and S3C, HEK293T cells (4 × 10^6/well) were seeded onto polylysine-coated 10 cm dishes and transiently transfected with 8µg of FLAG-XBP1u and 4µg of HA-Ubiquitin using 40 µl of PEI (1mg/ml). After 24 hours of transfection, cells were harvested in ice-cold 1x PBS. The cell pellet was resuspended in 300 µl of ribosome buffer (50mM Hepes, pH 7.4, 500mM KCl, 10mM MgCl2, 0.5% Triton X-100, 2.5u/ml of RNasin (Promega), and 1x PI) and incubated for 15 minutes on ice. Cell lysates were centrifuged at 20,000xg for 5 minutes. The resulting supernatant (200 µl) was carefully applied onto a 10% to 50% sucrose gradient and centrifuged for 1 hour at 55,000 rpm using a TLS-55 rotor at 4°C with the slowest acceleration and deceleration settings. After the centrifugation, 11 x 200 µl fractions were collected. 40 µl was directly analyzed by immunoblotting as input, while the remainder was diluted to 1 ml with RIPA buffer and immunoprecipitated using Rat anti-FLAG beads. The resulting immunoprecipitates were subsequently analyzed by immunoblotting.

To separate supernatants from ribosomes, as shown in Figures 3B and 6B, HEK293T cells (1.5 × 10^6/well) were seeded onto polylysine-coated 60 cm dishes and transiently transfected with 3µg

of FLAG-XBP1u or its mutants and 2μg of HA-Ubiquitin using 20μl of PEI (1mg/ml). After 24 hours of transfection, cells were washed once with 1xPBS and harvested in 1xPBS. The cell pellets were resuspended in 1ml of ribosome buffer and centrifuged for 5 minutes at 20,000xg at 4°C. 850μl of the supernatant was then centrifuged in a 1ml polycarbonate tube at 120,000xg for 40 minutes using a TLA120.2 rotor at 4°C. The supernatant was collected and adjusted to 0.1% SDS and 1% Triton X-100. The ribosomal pellet was washed with 200μl of ice-cold water and resuspended with 650μl of RIPA buffer. Both the supernatant and ribosome fractions were subjected to immunoprecipitation using anti-FLAG beads. The resulting immunoprecipitants were then analyzed by immunoblotting.

In vitro translation and ubiquitination.

In vitro transcription and translation were performed following established protocols[24,81] with the following modifications. PCR products encoding N-terminally FLAG-tagged XBP1u or its mutants were used as templates for in vitro transcription reactions. These PCR products were amplified from pCDNA5/FRT/TO FLAG-XBP1u constructs using a forward primer that included the Sp6 promoter sequence and annealed to the CMV promoter. The reverse primer annealed to the 3' end of XBP1u, excluding a stop codon for synthesizing XBP1u RNCs. For generating full-length PCR products, a reverse primer annealing to the poly A tail was used. In vitro transcription was performed using SP6 polymerase (New England Biolabs) and RNasin (Promega) at 37°C for 1.5 h. Transcripts lacking a stop codon were directly added to in vitro translation reactions, including hemin, nuclease-treated RRL, S35 methionine (PerkinElmer; #NEG009T005MC), and 10 μM His-tagged ubiquitin (Boston Biochem), and were incubated for 60 min at 32°C. Since transcripts lack a stop codon, ribosomes are stalled and subjected to ubiquitination by the RQC factors as shown previously[32]. The samples were kept on ice and an aliquot was withdrawn for direct analysis as input or denatured using 1% SDS (final concentration). The denatured samples were diluted to 1 ml with IP buffer (50mM Tris-HCl, 150mM NaCl, 1% Triton X-100) and subjected to pull down His-Ubiquitin conjugated XBP1u using Talon beads.

To demonstrate LTN1-mediated ubiquitination of XBP1u RNCs in Figure 4A, after translation for 60 minutes, the reactions were incubated with a buffer containing 20 μM MG132, 10 μM His-Ubiquitin, and an ATP regenerating system (1 mM ATP, 1 mM GTP, 12 mM creatine phosphate, 20 μg/ml creatine kinase), or concentrated cytosol prepared from WT HeLa or LKO cells, including 20 μM MG132, 10 μM His-Ubiquitin, and ATP regenerating system. The reactions were incubated for 60 minutes at 32°C. The samples were terminated by adjusting to 1% SDS and denatured by boiling, followed by dilution with 1 ml of IP buffer and pull down with Talon beads. For Figure 4B, after the 60-minute translation as above, the translation reactions were untreated, treated with 1 mM Puromycin, 1 μM E1 inhibitor (MLN4924)[52], or both, as indicated in the Figure 4 legends, and incubated for 30

minutes at 32°C. The samples were denatured, diluted, and pulled down with Talon beads as previously described. For Figure 4C, after puromycin treatment, samples were centrifuged at 120,000xg for 40 minutes using a TLA120.1 rotor before denaturation, dilution, and Talon pull down. For Figure 4D and 4E, the samples were withdrawn at different time points during the puromycin treatment, as indicated in the figure, and processed as above. For Figure 4F, the translation reactions were either left untreated, treated with 1 mM Puromycin, or treated with Puromycin along with 50μM PR-619. Samples were withdrawn at different time points for Talon pull down, as described above. For S4B, transcripts encoding full-length XBP1-AP* were translated for 60 minutes and incubated with either DMSO or 1 μM E1 inhibitor. The samples were aliquoted for the indicated time points and denatured and enriched for His-Ubiquitin conjugated proteins by Talon pull down. The Talon beads were boiled using 50 μl of 2x SDS sample buffer and analyzed along with inputs by SDS-PAGE followed by autoradiography.

Neutral PAGE and Phostag-based immunoblotting

HEK293T cells (0.125 × 10^6/well) were seeded onto polylysine-coated 24 well plates and transiently transfected with 0.4μg of HA-XBP1u or its mutants using 1μl of Lipofectamine-2000. After 24 hours of transfection, cells were directly harvested in 150ul of 2xSDS buffer prepared using RNAse free water and DTT. The samples were boiled for 10min and analyzed NuPAGE 4 to 12% Bis-Tris gel (Invitrogen) according to the manufacture recommendations. IRE1α phosphorylation was detected by previously described method[82]. Briefly, 5% SDS PAGE gel was made containing 25 μM Phos-tag (Wako). SDS-PAGE was run at 100 V for 2 hr and 40 min. The gel was transferred to nitrocellulose (Bio-Rad, Hercules, CA) and followed with western blotting.

Immunofluorescence

HEK293T cells were grown on polylysine-coated glass microscope slides in a 24 well plate. The cells were washed once with PBS and then fixed for 5 min with 3.7% formaldehyde in PBS. The fixed cells were washed twice with PBS and then permeabilized with 0.1% Triton X-100 in PBS. Cells were washed twice in PBS with 10% horse serum (HS) and 0.01% saponin and then blocked for 1 h in PBS/HS/saponin. Cells were incubated for 1 h with 1:100 dilution of Rat α-FLAG (BioLegend) in PBS/FBS/saponin and washed five times with PBS/HS/saponin for 5 min per wash. Cells were stained with a combination of goat α-RAT IgG-Cy2 (Jackson ImmunoResearch; #112–225-167) at 1:100 dilution in PBS/FBS/saponin in a dark place to avoid quenching of fluorophore. The cells were washed five times again, and the coverslips were mounted onto slides with Fluoromount G (SouthernBiotech; #0100–01). The mounting was allowed to set overnight at 4°C while covered. Confocal microscopy was performed on the slides using the Leica SP8 DMI6000 Confocal Microscope with a 63× oil objective,

1.40 aperture, and a PMT (photomultiplier tube) detector. Lasers at 488-nm wavelength was used to excite the Cy2 dye. Leica's LAS X software was used to capture and edit the gain, contrast, color, and scale bars of the images.

Quantification and statistical analysis

Quantification of autoradiographs were performed using ImageJ gel analysis. Error bars represent standard error of the mean (SEM) from two independent experiments as indicated in the figure legends. For data analysis in Figure 6C, the nuclear localization ratio of XBP1 was quantified using ImageJ. Firstly, the total fluorescence value of XBP1 for each cell was measured. Then, the nuclear area was circled to measure the fluorescence value within it. The nuclear localization ratio was calculated by dividing the nuclear area fluorescence value by the total cell value. Only cells with clear nuclear localization were included in the calculation.

References:

1. Wickner, S., Maurizi, M.R., and Gottesman, S. (1999). Posttranslational quality control: folding, refolding, and degrading proteins. Science *286*, 1888-1893. 10.1126/science.286.5446.1888.
2. Ross, C.A., and Poirier, M.A. (2004). Protein aggregation and neurodegenerative disease. Nature Medicine *10*, S10-S17. 10.1038/nm1066.
3. Ciechanover, A., and Kwon, Y.T. (2015). Degradation of misfolded proteins in neurodegenerative diseases: therapeutic targets and strategies. Exp Mol Med *47*, e147. 10.1038/emm.2014.117.
4. Wang, F., Durfee, L.A., and Huibregtse, J.M. (2013). A cotranslational ubiquitination pathway for quality control of misfolded proteins. Mol Cell *50*, 368-378. 10.1016/j.molcel.2013.03.009.
5. Duttler, S., Pechmann, S., and Frydman, J. (2013). Principles of cotranslational ubiquitination and quality control at the ribosome. Mol Cell *50*, 379-393. 10.1016/j.molcel.2013.03.010.
6. Sato, S., Ward, C.L., and Kopito, R.R. (1998). Cotranslational ubiquitination of cystic fibrosis transmembrane conductance regulator in vitro. J Biol Chem *273*, 7189-7192. 10.1074/jbc.273.13.7189.
7. Turner, G.C., and Varshavsky, A. (2000). Detecting and measuring cotranslational protein degradation in vivo. Science *289*, 2117-2120. 10.1126/science.289.5487.2117.
8. Vabulas, R.M., and Hartl, F.U. (2005). Protein synthesis upon acute nutrient restriction relies on proteasome function. Science *310*, 1960-1963. 10.1126/science.1121925.
9. Yewdell, J.W., and Nicchitta, C.V. (2006). The DRiP hypothesis decennial: support, controversy, refinement and extension. Trends Immunol *27*, 368-373. 10.1016/j.it.2006.06.008.
10. Pechmann, S., Willmund, F., and Frydman, J. (2013). The ribosome as a hub for protein quality control. Mol Cell *49*, 411-421. 10.1016/j.molcel.2013.01.020.
11. Princiotta, M.F., Finzi, D., Qian, S.B., Gibbs, J., Schuchmann, S., Buttgereit, F., Bennink, J.R., and Yewdell, J.W. (2003). Quantitating protein synthesis, degradation, and endogenous antigen processing. Immunity *18*, 343-354. 10.1016/s1074-7613(03)00051-7.

12. Bengtson, M.H., and Joazeiro, C.A. (2010). Role of a ribosome-associated E3 ubiquitin ligase in protein quality control. Nature *467*, 470-473. 10.1038/nature09371.
13. Brandman, O., and Hegde, R.S. (2016). Ribosome-associated protein quality control. Nat Struct Mol Biol *23*, 7-15. 10.1038/nsmb.3147.
14. Inada, T. (2020). Quality controls induced by aberrant translation. Nucleic Acids Res *48*, 1084-1096. 10.1093/nar/gkz1201.
15. Yip, M.C.J., and Shao, S. (2021). Detecting and Rescuing Stalled Ribosomes. Trends Biochem Sci *46*, 731-743. 10.1016/j.tibs.2021.03.008.
16. Brandman, O., Stewart-Ornstein, J., Wong, D., Larson, A., Williams, C.C., Li, G.W., Zhou, S., King, D., Shen, P.S., Weibezahn, J., et al. (2012). A ribosome-bound quality control complex triggers degradation of nascent peptides and signals translation stress. Cell *151*, 1042-1054. 10.1016/j.cell.2012.10.044.
17. Schuller, A.P., and Green, R. (2018). Roadblocks and resolutions in eukaryotic translation. Nat Rev Mol Cell Biol *19*, 526-541. 10.1038/s41580-018-0011-4.
18. Ito, K., and Chiba, S. (2013). Arrest peptides: cis-acting modulators of translation. Annu Rev Biochem *82*, 171-202. 10.1146/annurev-biochem-080211-105026.
19. Wilson, D.N., Arenz, S., and Beckmann, R. (2016). Translation regulation via nascent polypeptide-mediated ribosome stalling. Curr Opin Struct Biol *37*, 123-133. 10.1016/j.sbi.2016.01.008.
20. Ingolia, N.T., Lareau, L.F., and Weissman, J.S. (2011). Ribosome profiling of mouse embryonic stem cells reveals the complexity and dynamics of mammalian proteomes. Cell *147*, 789-802. 10.1016/j.cell.2011.10.002.
21. Han, P., Shichino, Y., Schneider-Poetsch, T., Mito, M., Hashimoto, S., Udagawa, T., Kohno, K., Yoshida, M., Mishima, Y., Inada, T., and Iwasaki, S. (2020). Genome-wide Survey of Ribosome Collision. Cell Rep *31*, 107610. 10.1016/j.celrep.2020.107610.
22. Lu, J., and Deutsch, C. (2008). Electrostatics in the ribosomal tunnel modulate chain elongation rates. J Mol Biol *384*, 73-86. 10.1016/j.jmb.2008.08.089.
23. Stein, K.C., Morales-Polanco, F., van der Lienden, J., Rainbolt, T.K., and Frydman, J. (2022). Ageing exacerbates ribosome pausing to disrupt cotranslational proteostasis. Nature *601*, 637-642. 10.1038/s41586-021-04295-4.
24. Mariappan, M., Li, X., Stefanovic, S., Sharma, A., Mateja, A., Keenan, R.J., and Hegde, R.S. (2010). A ribosome-associating factor chaperones tail-anchored membrane proteins. Nature *466*, 1120-1124. 10.1038/nature09296.
25. Collart, M.A., and Weiss, B. (2020). Ribosome pausing, a dangerous necessity for co-translational events. Nucleic Acids Res *48*, 1043-1055. 10.1093/nar/gkz763.
26. Yanagitani, K., Kimata, Y., Kadokura, H., and Kohno, K. (2011). Translational pausing ensures membrane targeting and cytoplasmic splicing of XBP1u mRNA. Science *331*, 586-589. 10.1126/science.1197142.
27. Sepulveda, G., Antkowiak, M., Brust-Mascher, I., Mahe, K., Ou, T., Castro, N.M., Christensen, L.N., Cheung, L., Jiang, X., Yoon, D., et al. (2018). Co-translational protein targeting facilitates centrosomal recruitment of PCNT during centrosome maturation in vertebrates. Elife *7*. 10.7554/eLife.34959.

28. Zhao, T., Chen, Y.M., Li, Y., Wang, J., Chen, S., Gao, N., and Qian, W. (2021). Disome-seq reveals widespread ribosome collisions that promote cotranslational protein folding. Genome Biol *22*, 16. 10.1186/s13059-020-02256-0.
29. Joazeiro, C.A.P. (2019). Mechanisms and functions of ribosome-associated protein quality control. Nat Rev Mol Cell Biol *20*, 368-383. 10.1038/s41580-019-0118-2.
30. Howard, C.J., and Frost, A. (2021). Ribosome-associated quality control and CAT tailing. Crit Rev Biochem Mol Biol *56*, 603-620. 10.1080/10409238.2021.1938507.
31. D'Orazio, K.N., and Green, R. (2021). Ribosome states signal RNA quality control. Mol Cell *81*, 1372-1383. 10.1016/j.molcel.2021.02.022.
32. Shao, S., von der Malsburg, K., and Hegde, R.S. (2013). Listerin-dependent nascent protein ubiquitination relies on ribosome subunit dissociation. Mol Cell *50*, 637-648. 10.1016/j.molcel.2013.04.015.
33. Shoemaker, C.J., Eyler, D.E., and Green, R. (2010). Dom34:Hbs1 promotes subunit dissociation and peptidyl-tRNA drop-off to initiate no-go decay. Science *330*, 369-372. 10.1126/science.1192430.
34. Pisareva, V.P., Skabkin, M.A., Hellen, C.U., Pestova, T.V., and Pisarev, A.V. (2011). Dissociation by Pelota, Hbs1 and ABCE1 of mammalian vacant 80S ribosomes and stalled elongation complexes. Embo j *30*, 1804-1817. 10.1038/emboj.2011.93.
35. Lyumkis, D., Oliveira dos Passos, D., Tahara, E.B., Webb, K., Bennett, E.J., Vinterbo, S., Potter, C.S., Carragher, B., and Joazeiro, C.A. (2014). Structural basis for translational surveillance by the large ribosomal subunit-associated protein quality control complex. Proc Natl Acad Sci U S A *111*, 15981-15986. 10.1073/pnas.1413882111.
36. Shen, P.S., Park, J., Qin, Y., Li, X., Parsawar, K., Larson, M.H., Cox, J., Cheng, Y., Lambowitz, A.M., Weissman, J.S., et al. (2015). Protein synthesis. Rqc2p and 60S ribosomal subunits mediate mRNA-independent elongation of nascent chains. Science *347*, 75-78. 10.1126/science.1259724.
37. Defenouillère, Q., Yao, Y., Mouaikel, J., Namane, A., Galopier, A., Decourty, L., Doyen, A., Malabat, C., Saveanu, C., Jacquier, A., and Fromont-Racine, M. (2013). Cdc48-associated complex bound to 60S particles is required for the clearance of aberrant translation products. Proc Natl Acad Sci U S A *110*, 5046-5051. 10.1073/pnas.1221724110.
38. von der Malsburg, K., Shao, S., and Hegde, R.S. (2015). The ribosome quality control pathway can access nascent polypeptides stalled at the Sec61 translocon. Mol Biol Cell *26*, 2168-2180. 10.1091/mbc.E15-01-0040.
39. Arakawa, S., Yunoki, K., Izawa, T., Tamura, Y., Nishikawa, S., and Endo, T. (2016). Quality control of nonstop membrane proteins at the ER membrane and in the cytosol. Sci Rep *6*, 30795. 10.1038/srep30795.
40. Buchanan, B.W., Mehrtash, A.B., Broshar, C.L., Runnebohm, A.M., Snow, B.J., Scanameo, L.N., Hochstrasser, M., and Rubenstein, E.M. (2019). Endoplasmic reticulum stress differentially inhibits endoplasmic reticulum and inner nuclear membrane protein quality control degradation pathways. J Biol Chem *294*, 19814-19830. 10.1074/jbc.RA119.010295.
41. Trentini, D.B., Pecoraro, M., Tiwary, S., Cox, J., Mann, M., Hipp, M.S., and Hartl, F.U. (2020). Role for ribosome-associated quality control in sampling proteins for MHC class I-mediated antigen presentation. Proc Natl Acad Sci U S A *117*, 4099-4108. 10.1073/pnas.1914401117.

42. Verma, R., Oania, R.S., Kolawa, N.J., and Deshaies, R.J. (2013). Cdc48/p97 promotes degradation of aberrant nascent polypeptides bound to the ribosome. Elife *2*, e00308. 10.7554/eLife.00308.
43. Ito-Harashima, S., Kuroha, K., Tatematsu, T., and Inada, T. (2007). Translation of the poly(A) tail plays crucial roles in nonstop mRNA surveillance via translation repression and protein destabilization by proteasome in yeast. Genes Dev *21*, 519-524. 10.1101/gad.1490207.
44. Yoshida, H., Matsui, T., Yamamoto, A., Okada, T., and Mori, K. (2001). XBP1 mRNA is induced by ATF6 and spliced by IRE1 in response to ER stress to produce a highly active transcription factor. Cell *107*, 881-891. 10.1016/s0092-8674(01)00611-0.
45. Calfon, M., Zeng, H., Urano, F., Till, J.H., Hubbard, S.R., Harding, H.P., Clark, S.G., and Ron, D. (2002). IRE1 couples endoplasmic reticulum load to secretory capacity by processing the XBP-1 mRNA. Nature *415*, 92-96. 10.1038/415092a.
46. Yanagitani, K., Imagawa, Y., Iwawaki, T., Hosoda, A., Saito, M., Kimata, Y., and Kohno, K. (2009). Cotranslational targeting of XBP1 protein to the membrane promotes cytoplasmic splicing of its own mRNA. Mol Cell *34*, 191-200. 10.1016/j.molcel.2009.02.033.
47. Shanmuganathan, V., Schiller, N., Magoulopoulou, A., Cheng, J., Braunger, K., Cymer, F., Berninghausen, O., Beatrix, B., Kohno, K., von Heijne, G., and Beckmann, R. (2019). Structural and mutational analysis of the ribosome-arresting human XBP1u. Elife *8*. 10.7554/eLife.46267.
48. Plumb, R., Zhang, Z.R., Appathurai, S., and Mariappan, M. (2015). A functional link between the co-translational protein translocation pathway and the UPR. Elife *4*. 10.7554/eLife.07426.
49. Kanda, S., Yanagitani, K., Yokota, Y., Esaki, Y., and Kohno, K. (2016). Autonomous translational pausing is required for XBP1u mRNA recruitment to the ER via the SRP pathway. Proc Natl Acad Sci U S A *113*, E5886-e5895. 10.1073/pnas.1604435113.
50. Chen, C.Y., Malchus, N.S., Hehn, B., Stelzer, W., Avci, D., Langosch, D., and Lemberg, M.K. (2014). Signal peptide peptidase functions in ERAD to cleave the unfolded protein response regulator XBP1u. Embo j *33*, 2492-2506. 10.15252/embj.201488208.
51. Azzam, M.E., and Algranati, I.D. (1973). Mechanism of puromycin action: fate of ribosomes after release of nascent protein chains from polysomes. Proc Natl Acad Sci U S A *70*, 3866-3869. 10.1073/pnas.70.12.3866.
52. Soucy, T.A., Smith, P.G., Milhollen, M.A., Berger, A.J., Gavin, J.M., Adhikari, S., Brownell, J.E., Burke, K.E., Cardin, D.P., Critchley, S., et al. (2009). An inhibitor of NEDD8-activating enzyme as a new approach to treat cancer. Nature *458*, 732-736. 10.1038/nature07884.
53. Altun, M., Kramer, H.B., Willems, L.I., McDermott, J.L., Leach, C.A., Goldenberg, S.J., Kumar, K.G., Konietzny, R., Fischer, R., Kogan, E., et al. (2011). Activity-based chemical proteomics accelerates inhibitor development for deubiquitylating enzymes. Chem Biol *18*, 1401-1412. 10.1016/j.chembiol.2011.08.018.
54. Hessa, T., Sharma, A., Mariappan, M., Eshleman, H.D., Gutierrez, E., and Hegde, R.S. (2011). Protein targeting and degradation are coupled for elimination of mislocalized proteins. Nature *475*, 394-397. 10.1038/nature10181.
55. Rodrigo-Brenni, M.C., Gutierrez, E., and Hegde, R.S. (2014). Cytosolic quality control of mislocalized proteins requires RNF126 recruitment to Bag6. Mol Cell *55*, 227-237. 10.1016/j.molcel.2014.05.025.
56. Banaszynski, L.A., Chen, L.C., Maynard-Smith, L.A., Ooi, A.G., and Wandless, T.J. (2006). A rapid, reversible, and tunable method to regulate protein function in living cells using synthetic small molecules. Cell *126*, 995-1004. 10.1016/j.cell.2006.07.025.

57. Yoshida, H., Uemura, A., and Mori, K. (2009). pXBP1(U), a negative regulator of the unfolded protein response activator pXBP1(S), targets ATF6 but not ATF4 in proteasome-mediated degradation. Cell Struct Funct *34*, 1-10. 10.1247/csf.06028.
58. Li, X., Sun, S., Appathurai, S., Sundaram, A., Plumb, R., and Mariappan, M. (2020). A Molecular Mechanism for Turning Off IRE1α Signaling during Endoplasmic Reticulum Stress. Cell Rep *33*, 108563. 10.1016/j.celrep.2020.108563.
59. Thrower, J.S., Hoffman, L., Rechsteiner, M., and Pickart, C.M. (2000). Recognition of the polyubiquitin proteolytic signal. Embo j *19*, 94-102. 10.1093/emboj/19.1.94.
60. Thrun, A., Garzia, A., Kigoshi-Tansho, Y., Patil, P.R., Umbaugh, C.S., Dallinger, T., Liu, J., Kreger, S., Patrizi, A., Cox, G.A., et al. (2021). Convergence of mammalian RQC and C-end rule proteolytic pathways via alanine tailing. Mol Cell *81*, 2112-2122.e2117. 10.1016/j.molcel.2021.03.004.
61. Tesina, P., Ebine, S., Buschauer, R., Thoms, M., Matsuo, Y., Inada, T., and Beckmann, R. (2023). Molecular basis of eIF5A-dependent CAT tailing in eukaryotic ribosome-associated quality control. Mol Cell *83*, 607-621.e604. 10.1016/j.molcel.2023.01.020.
62. Sitron, C.S., and Brandman, O. (2019). CAT tails drive degradation of stalled polypeptides on and off the ribosome. Nat Struct Mol Biol *26*, 450-459. 10.1038/s41594-019-0230-1.
63. Verma, R., Reichermeier, K.M., Burroughs, A.M., Oania, R.S., Reitsma, J.M., Aravind, L., and Deshaies, R.J. (2018). Vms1 and ANKZF1 peptidyl-tRNA hydrolases release nascent chains from stalled ribosomes. Nature *557*, 446-451. 10.1038/s41586-018-0022-5.
64. Yip, M.C.J., Keszei, A.F.A., Feng, Q., Chu, V., McKenna, M.J., and Shao, S. (2019). Mechanism for recycling tRNAs on stalled ribosomes. Nat Struct Mol Biol *26*, 343-349. 10.1038/s41594-019-0211-4.
65. Kuroha, K., Zinoviev, A., Hellen, C.U.T., and Pestova, T.V. (2018). Release of Ubiquitinated and Non-ubiquitinated Nascent Chains from Stalled Mammalian Ribosomal Complexes by ANKZF1 and Ptrh1. Mol Cell *72*, 286-302.e288. 10.1016/j.molcel.2018.08.022.
66. Zhang, Z.R., Bonifacino, J.S., and Hegde, R.S. (2013). Deubiquitinases sharpen substrate discrimination during membrane protein degradation from the ER. Cell *154*, 609-622. 10.1016/j.cell.2013.06.038.
67. Helenius, A., and Aebi, M. (2004). Roles of N-linked glycans in the endoplasmic reticulum. Annu Rev Biochem *73*, 1019-1049. 10.1146/annurev.biochem.73.011303.073752.
68. Lu, Y., Lee, B.H., King, R.W., Finley, D., and Kirschner, M.W. (2015). Substrate degradation by the proteasome: a single-molecule kinetic analysis. Science *348*, 1250834. 10.1126/science.1250834.
69. Pierce, N.W., Kleiger, G., Shan, S.O., and Deshaies, R.J. (2009). Detection of sequential polyubiquitylation on a millisecond timescale. Nature *462*, 615-619. 10.1038/nature08595.
70. Vembar, S.S., and Brodsky, J.L. (2008). One step at a time: endoplasmic reticulum-associated degradation. Nat Rev Mol Cell Biol *9*, 944-957. 10.1038/nrm2546.
71. Hu, X., Wang, L., Wang, Y., Ji, J., Li, J., Wang, Z., Li, C., Zhang, Y., and Zhang, Z.R. (2020). RNF126-Mediated Reubiquitination Is Required for Proteasomal Degradation of p97-Extracted Membrane Proteins. Mol Cell *79*, 320-331.e329. 10.1016/j.molcel.2020.06.023.
72. Leto, D.E., Morgens, D.W., Zhang, L., Walczak, C.P., Elias, J.E., Bassik, M.C., and Kopito, R.R. (2019). Genome-wide CRISPR Analysis Identifies Substrate-Specific Conjugation Modules in ER-Associated Degradation. Mol Cell *73*, 377-389.e311. 10.1016/j.molcel.2018.11.015.

73. Bernardi, K.M., Forster, M.L., Lencer, W.I., and Tsai, B. (2008). Derlin-1 facilitates the retro-translocation of cholera toxin. Mol Biol Cell *19*, 877-884. 10.1091/mbc.e07-08-0755.
74. Byun, H., Halani, N., Mertz, J.A., Ali, A.F., Lozano, M.M., and Dudley, J.P. (2010). Retroviral Rem protein requires processing by signal peptidase and retrotranslocation for nuclear function. Proc Natl Acad Sci U S A *107*, 12287-12292. 10.1073/pnas.1004303107.
75. Eshraghi, M., Karunadharma, P.P., Blin, J., Shahani, N., Ricci, E.P., Michel, A., Urban, N.T., Galli, N., Sharma, M., Ramírez-Jarquín, U.N., et al. (2021). Mutant Huntingtin stalls ribosomes and represses protein synthesis in a cellular model of Huntington disease. Nat Commun *12*, 1461. 10.1038/s41467-021-21637-y.
76. Yang, J., Hao, X., Cao, X., Liu, B., and Nyström, T. (2016). Spatial sequestration and detoxification of Huntingtin by the ribosome quality control complex. Elife *5*. 10.7554/eLife.11792.
77. Sundaram, A., Appathurai, S., Plumb, R., and Mariappan, M. (2018). Dynamic changes in complexes of IRE1α, PERK, and ATF6α during endoplasmic reticulum stress. Mol Biol Cell *29*, 1376-1388. 10.1091/mbc.E17-10-0594.
78. Mali, P., Yang, L., Esvelt, K.M., Aach, J., Guell, M., DiCarlo, J.E., Norville, J.E., and Church, G.M. (2013). RNA-guided human genome engineering via Cas9. Science *339*, 823-826. 10.1126/science.1232033.
79. Ran, F.A., Hsu, P.D., Wright, J., Agarwala, V., Scott, D.A., and Zhang, F. (2013). Genome engineering using the CRISPR-Cas9 system. Nat Protoc *8*, 2281-2308. 10.1038/nprot.2013.143.
80. Labun, K., Montague, T.G., Krause, M., Torres Cleuren, Y.N., Tjeldnes, H., and Valen, E. (2019). CHOPCHOP v3: expanding the CRISPR web toolbox beyond genome editing. Nucleic Acids Res *47*, W171-w174. 10.1093/nar/gkz365.
81. Sharma, A., Mariappan, M., Appathurai, S., and Hegde, R.S. (2010). In vitro dissection of protein translocation into the mammalian endoplasmic reticulum. Methods Mol Biol *619*, 339-363. 10.1007/978-1-60327-412-8_20.
82. Yang, L., Xue, Z., He, Y., Sun, S., Chen, H., and Qi, L. (2010). A Phos-tag-based approach reveals the extent of physiological endoplasmic reticulum stress. PLoS One *5*, e11621. 10.1371/journal.pone.0011621.

Figure 1

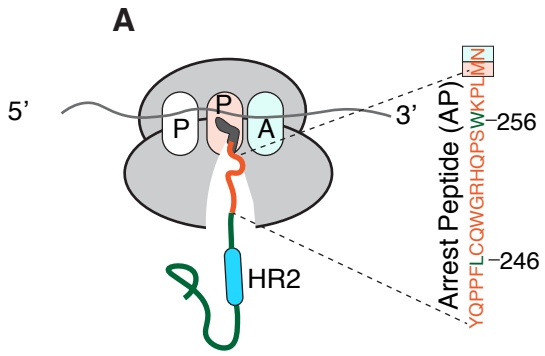
A
5'
3'
P
P
A
HR2
Arrest Peptide (AP)
YQPPFLCQWGRHQPSWKPLMN
256
246

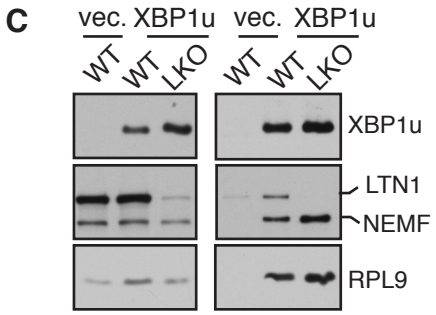
C
vec. XBP1u vec. XBP1u
WT WT LKO WT WT LKO
XBP1u
LTN1
NEMF
RPL9

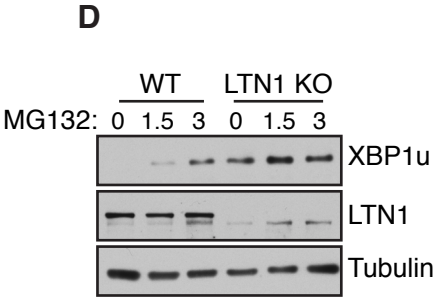
D
WT LTN1 KO
MG132: 0 1.5 3 0 1.5 3
XBP1u
LTN1
Tubulin

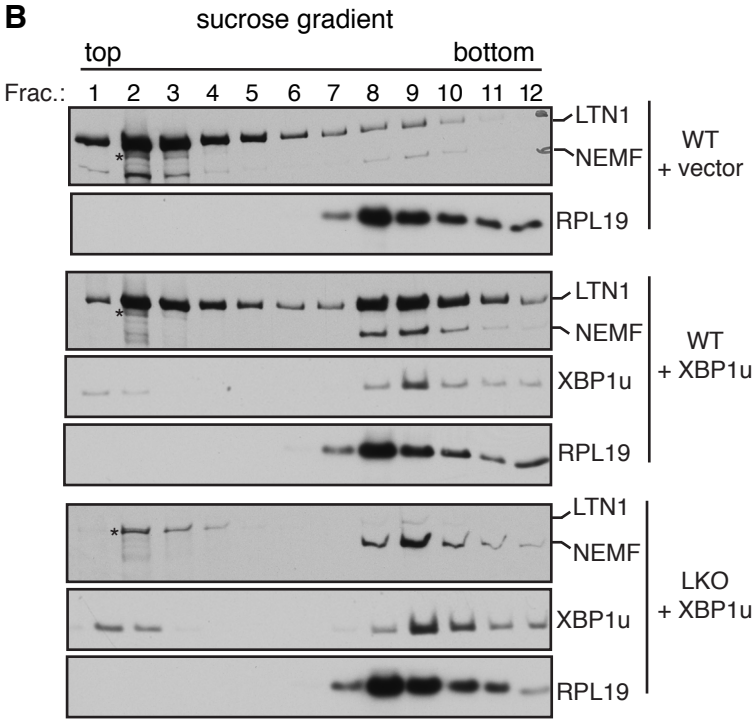
B
sucrose gradient
top
bottom
Frac.: 1 2 3 4 5 6 7 8 9 10 11 12
LTN1
NEMF
RPL19
WT + vector
LTN1
NEMF
XBP1u
RPL19
WT + XBP1u
LTN1
NEMF
XBP1u
RPL19
LKO + XBP1u

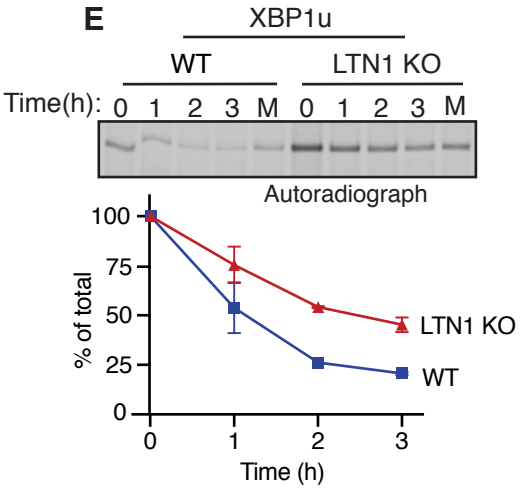
E
XBP1u
WT
LTN1 KO
Time(h): 0 1 2 3 M 0 1 2 3 M
Autoradiograph
100
75
50
25
0
% of total
LTN1 KO
WT
0 1 2 3
Time (h)

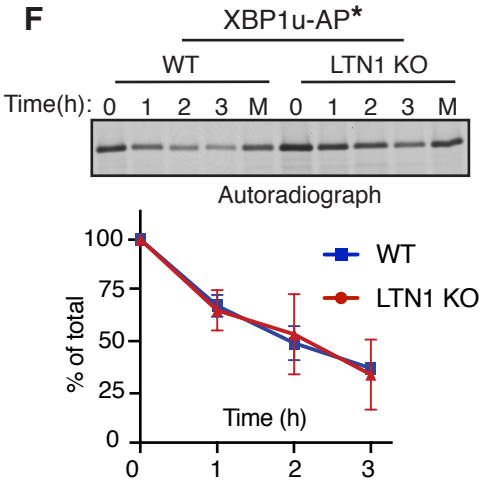
F
XBP1u-AP*
WT
LTN1 KO
Time(h): 0 1 2 3 M 0 1 2 3 M
Autoradiograph
100
75
50
25
0
% of total
WT
LTN1 KO
Time (h)
0 1 2 3

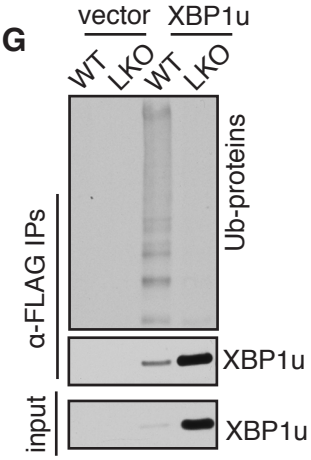
G
vector XBP1u
WT LKO WT LKO
α-FLAG IPs
Ub-proteins
XBP1u
input
XBP1u

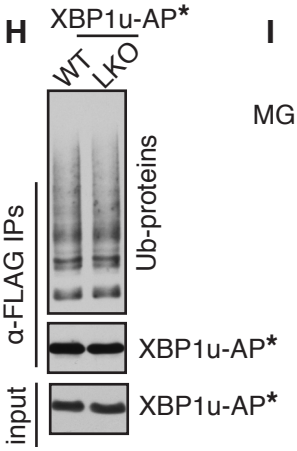
H
XBP1u-AP*
WT LKO
α-FLAG IPs
Ub-proteins
XBP1u-AP*
input
XBP1u-AP*

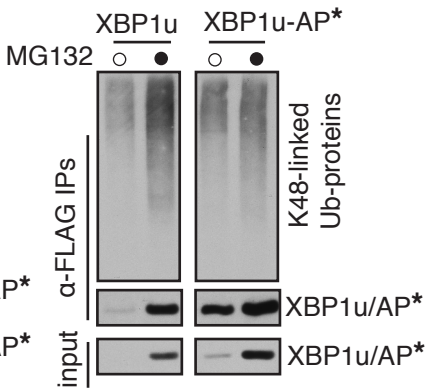
I
XBP1u XBP1u-AP*
MG132 ○ ● ○ ●
α-FLAG IPs
K48-linked Ub-proteins
XBP1u/AP*
input
XBP1u/AP*

Figure 1. LTN1 mediates ubiquitination of nascent chains on translationally stalled ribosomes in cells.

(A) A schematic diagram illustrates the ribosome stalling induced by XBP1u arrest peptide (AP). The incorporation of the last asparagine (N) residue is inhibited due to the stall. The mutation of L246 and W256 to alanine residues relieves the stall.

(B) WT 293T cells or LTN1 KO (LKO) cells expressing empty vector or XBP1u were fractionated by 10-30% sucrose density gradient and the fractions were analyzed by immunoblotting for the indicated antigens.

(C) Cells expressing empty vector or FLAG-tagged XBP1u were lysed and immunoprecipitated (IPed) for XBP1u using anti-FLAG beads and analyzed by immunoblotting.

(D) WT and LKO cells were treated with MG132 (20μM) for the indicated time points and analyzed by immunoblotting.

(E, F) Pulse-chase analysis of WT and LKO cells expressing XBP1u or XBP1u-AP*. The data were quantified from two independent experiments are represented as means ±SEMs.

(G) Empty vector or FLAG-XBP1u is transfected along with HA-ubiquitin into WT or LKO cells were immunoprecipitated with anti-FLAG beads. The resulting samples were probed for ubiquitinated proteins (Ub-proteins) using an HA antibody and for XBP1u with an anti-FLAG antibody.

(H) The indicated cells expressing FLAG-XBP1u-AP* were analyzed as in (G).

(I) Cells expressing FLAG-XBP1u or FLAG-XBP1u-AP were analyzed as in (G), but IP samples were probed with an K48-linked ubiquitin chain specific antibody.

See also **Figure S1**

Figure 2

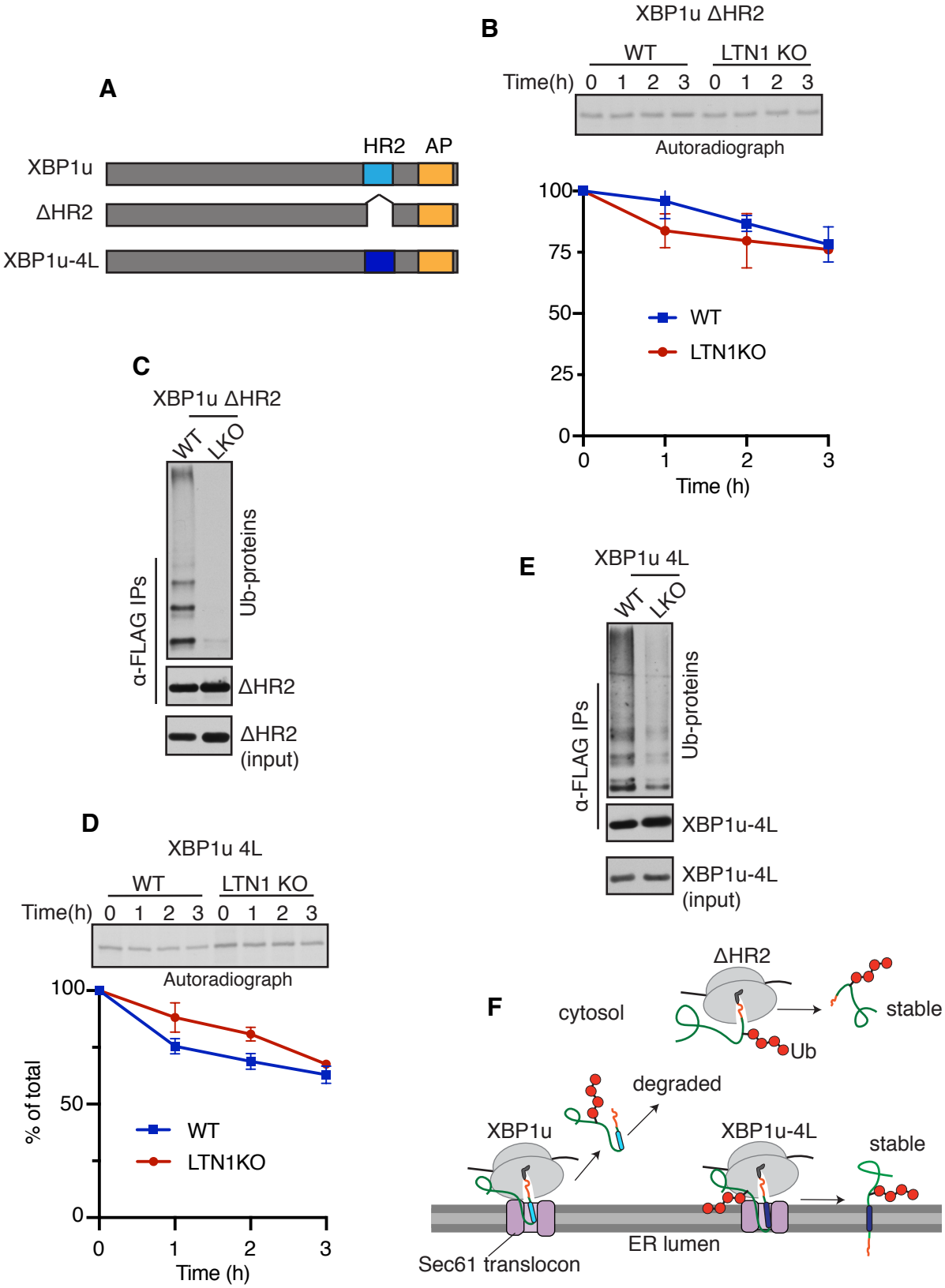
A
HR2
AP
XBP1u
ΔHR2
XBP1u-4L
B
XBP1u ΔHR2
WT
LTN1 KO
Time(h) 0 1 2 3 0 1 2 3
Autoradiograph
100
75
50
25
0
WT
LTN1KO
0 1 2 3
Time (h)
C
XBP1u ΔHR2
WT
LKO
α-FLAG IPs
Ub-proteins
ΔHR2
ΔHR2 (input)
D
XBP1u 4L
WT
LTN1 KO
Time(h) 0 1 2 3 0 1 2 3
Autoradiograph
100
50
0
% of total
WT
LTN1KO
0 1 2 3
Time (h)
E
XBP1u 4L
WT
LKO
α-FLAG IPs
Ub-proteins
XBP1u-4L
XBP1u-4L (input)
F
cytosol
ΔHR2
stable
Ub
degraded
XBP1u
XBP1u-4L
stable
ER lumen
Sec61 translocon

Figure 2. Nascent chain ubiquitination by LTN1 is insufficient for proteasomal degradation

(A) Cartoon illustrating WT XBP1u, XBP1u lacking Hydrophobic Region 2 (HR2), and XBP1u-4L with four hydrophobic leucine residues replacing four less hydrophobic residues in HR2.

(B) Pulse-chase analysis of WT and LKO cells expressing XBP1uΔHR2. The data were quantified from two independent experiments are represented as means ±SEMs.

(C) FLAG-XBP1uΔHR2 transfected along with HA-ubiquitin into WT or LKO cells were immunoprecipitated with anti-FLAG beads and probed for ubiquitinated proteins (Ub-proteins) using an HA antibody and for XBP1uΔHR2 with an anti-FLAG antibody.

(D) WT and LKO cells expressing XBP1u 4L were analyzed by pulse chase as in (B).

(E) The indicated XBP1u 4L expressing cells were analyzed as in (C)

(F) Schematic diagram depicting the critical role of exposed hydrophobicity in XBPu in mediating proteasomal degradation.

See also **Figure S2**

Figure 3

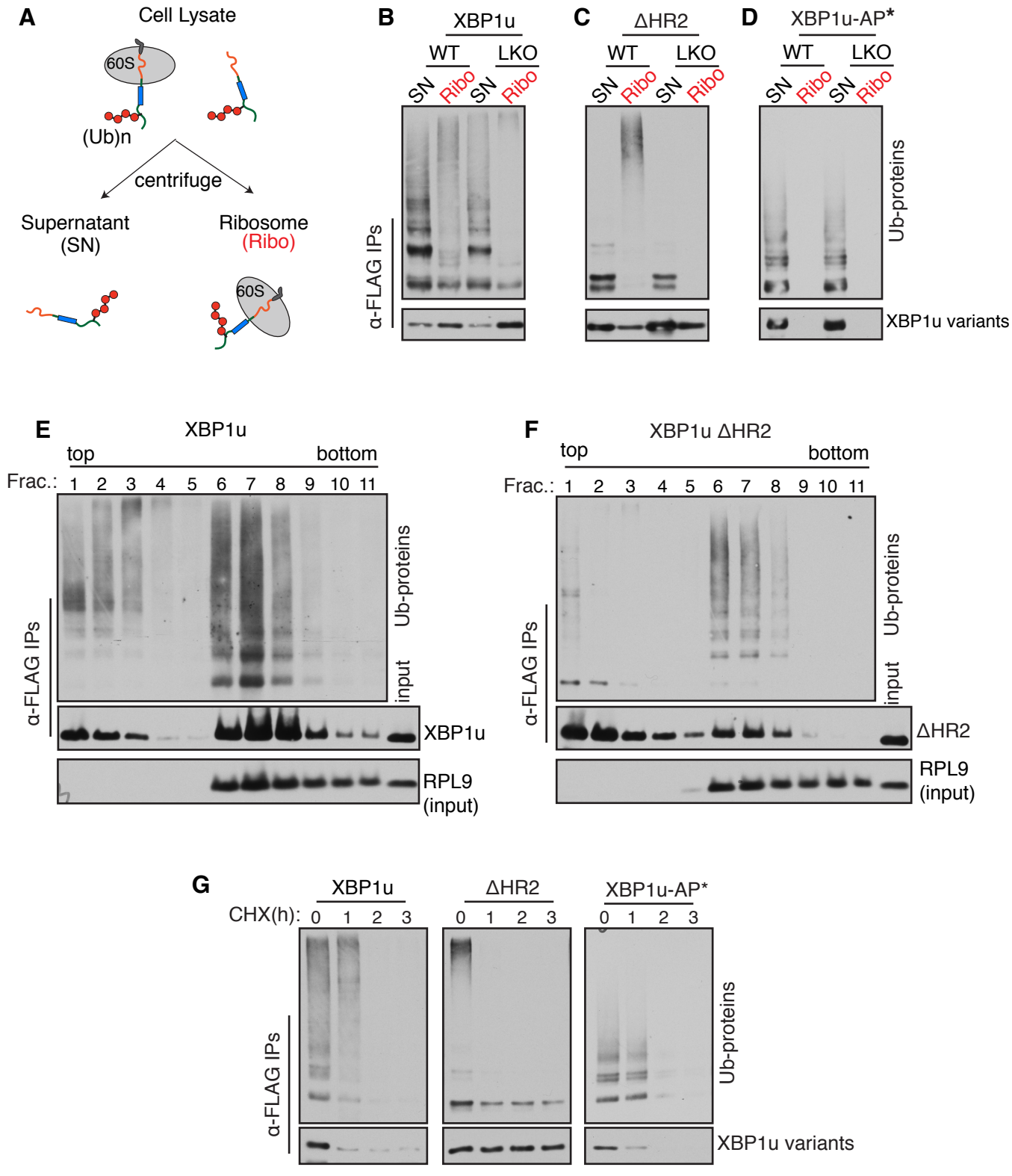
A
Cell Lysate
60S
(Ub)n
centrifuge
Supernatant
(SN)
Ribosome
(Ribo)
60S
B
XBP1u
WT
LKO
SN
Ribo
SN
Ribo
α-FLAG IPs
C
ΔHR2
WT
LKO
SN
Ribo
SN
Ribo
D
XBP1u-AP*
WT
LKO
SN
Ribo
SN
Ribo
Ub-proteins
XBP1u variants
E
XBP1u
top
bottom
Frac.: 1 2 3 4 5 6 7 8 9 10 11
α-FLAG IPs
Ub-proteins
input
XBP1u
RPL9
(input)
F
XBP1u ΔHR2
top
bottom
Frac.: 1 2 3 4 5 6 7 8 9 10 11
α-FLAG IPs
Ub-proteins
input
ΔHR2
RPL9
(input)
G
XBP1u
ΔHR2
XBP1u-AP*
CHX(h): 0 1 2 3
0 1 2 3
0 1 2 3
α-FLAG IPs
Ub-proteins
XBP1u variants

Figure 3. Nascent chains ubiquitinated by LTN1 is deubiquitinated in the cytosol

(A) Schematic depicting the separation of ribosome-associated nascent chains from free nascent chains in the supernatant through ultracentrifugation.

(B, C, D) WT and LKO cells expressing the indicated XBP1u variant along with HA-ubiquitin were separated into supernatants and ribosome pellets. The resulting samples were immunoprecipitated using anti-FLAG beads and probed for Ub-proteins using an HA antibody. The presence of XBP1u variants were probed with an anti-FLAG antibody.

(E, F) Cell lysates of XBP1u or XBP1uΔHR2 were subjected to a 10-50% sucrose density gradient. Input fractions were directly probed for the ribosomal protein RPL9, while XBP1u and its mutant were IPed using anti-FLAG beads and analyzed by immunoblotting.

(G). Cells expressing the specified variant of XBP1u alongside HA-ubiquitin were treated with cycloheximide and collected at the indicated time points. The samples were subjected to anti-FLAG IP and were probed for Ub-proteins using an HA antibody. XBPu and its mutants were detected using anti-FLAG antibodies.

See also **Figure S3**

Figure 4

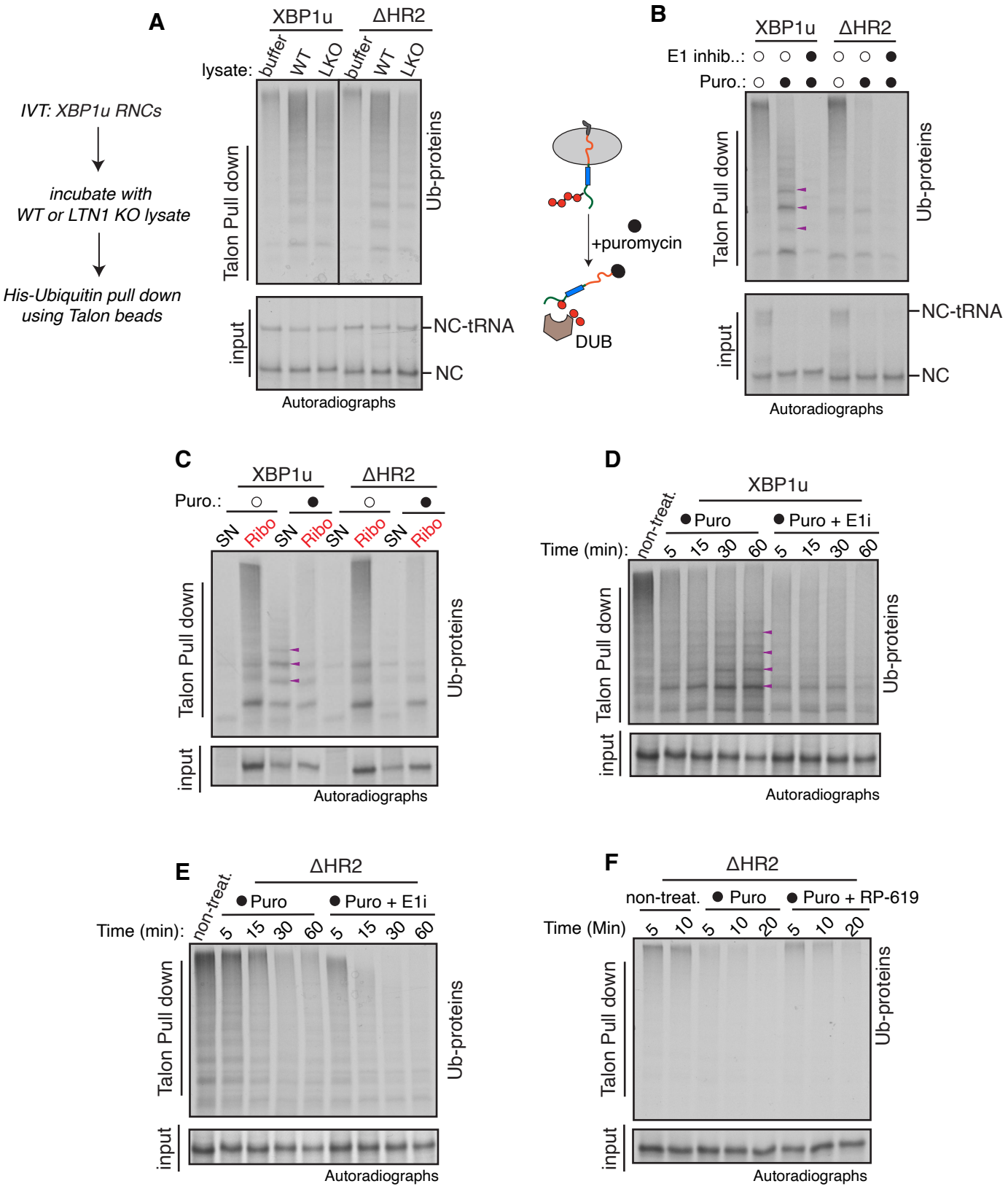
A
XBP1u
ΔHR2
lysate: buffer WT LKO buffer WT LKO
IVT: XBP1u RNCs
incubate with WT or LTN1 KO lysate
His-Ubiquitin pull down using Talon beads
Talon Pull down
Ub-proteins
input
NC-tRNA
NC
Autoradiographs
+puromycin
DUB
B
E1 inhib..:
Puro.:
C
SN Ribo SN Ribo SN Ribo SN Ribo
D
non-treat.
Puro
Puro + E1i
Time (min): 5 15 30 60 5 15 30 60
E
F
Puro + RP-619
Time (Min) 5 10 5 10 20 5 10 20

Figure 4. Nascent chain is deubiquitinated after its dissociation from the ribosome

(A) The indicated versions of XBP1u transcripts lacking a termination codon were translated in rabbit reticulocyte lysate (RRL) supplemented with 35S-methionine and His-Ubiquitin. The reactions containing ribosome-associated nascent chains (RNCs) were incubated with a buffer or the cytosol from WT 293T or LKO cells. The samples were then denatured and either directly analyzed as input or subjected to Talon pull-down to capture His-ubiquitin-conjugated radiolabeled XBP1u. The resulting samples were visualized by autoradiography. Notably, tRNA-attached nascent chains (NC) were preserved during SDS/PAGE electrophoresis.

(B) Ubiquitinated RNCs of XBP1u and its mutant were prepared as in B and and subsequently treated with puromycin for 45 minutes. An E1 inhibitor (MLN4924) was included along with puromycin. The samples were then denatured and analyzed as in (A).

(C) The reactions were performed as described in (B), with subsequent analysis conducted after separating supernatants from ribosomes through ultracentrifugation.

(D, E) Ubiquitinated RNCs were prepared and analyzed as described in (B), with samples collected at various time points during the incubation for subsequent analysis.

(F) Ubiquitinated RNCs of XBP1uΔHR2 were prepared and analyzed as in (B), with the addition of a generic DUB inhibitor PR-619 in one set of reactions during puromycin treatment.

See also **Figure S4**

Figure 5

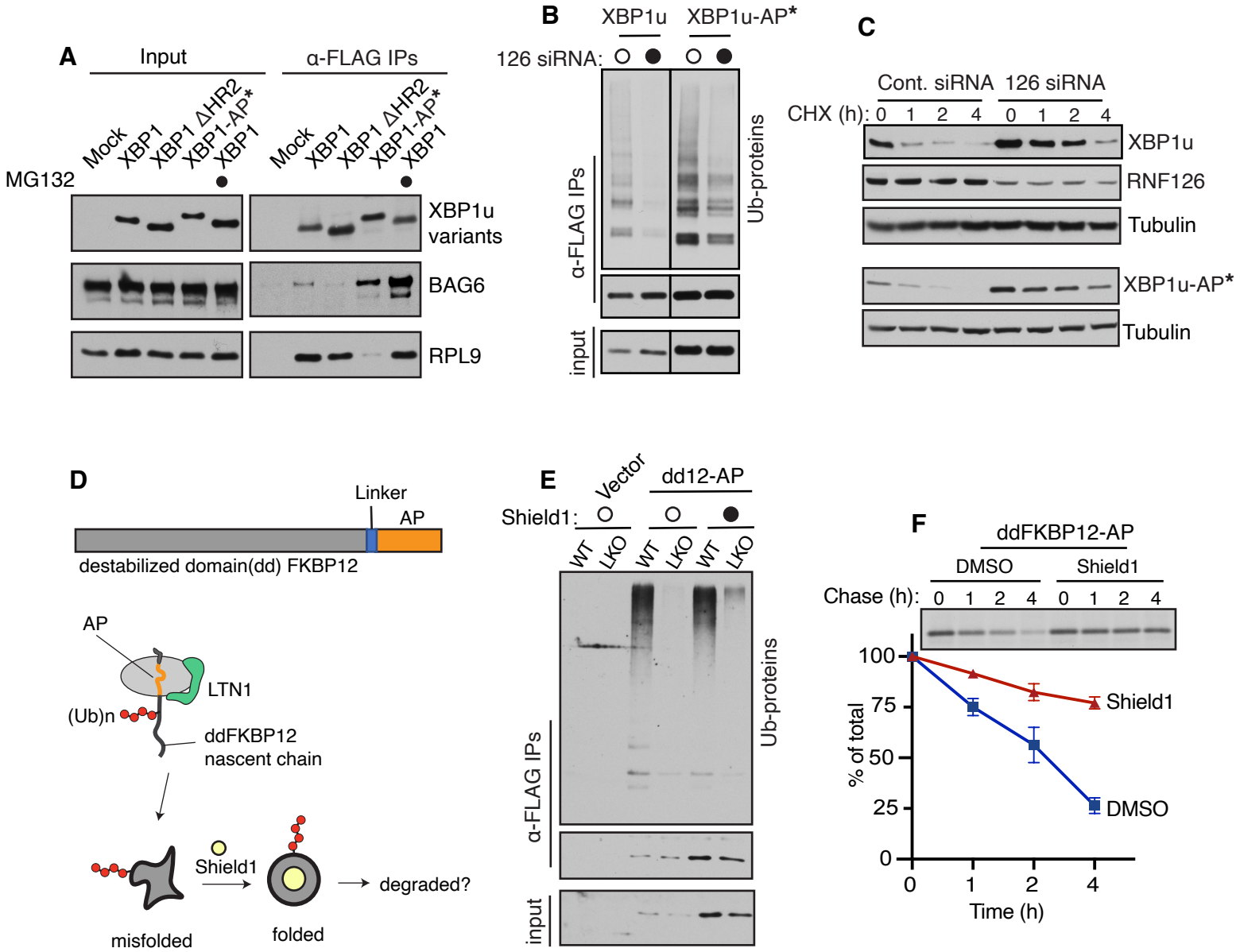
A
Input
α-FLAG IPs
Mock
XBP1
XBP1 ΔHR2
XBP1-AP*
XBP1
MG132
XBP1u variants
BAG6
RPL9
B
XBP1u
XBP1u-AP*
126 siRNA:
α-FLAG IPs
Ub-proteins
input
C
Cont. siRNA
126 siRNA
CHX (h): 0 1 2 4 0 1 2 4
XBP1u
RNF126
Tubulin
XBP1u-AP*
Tubulin
D
Linker
AP
destabilized domain(dd) FKBP12
AP
LTN1
(Ub)n
ddFKBP12
nascent chain
Shield1
degraded?
misfolded
folded
E
Vector
dd12-AP
Shield1:
WT
LKO
WT
LKO
WT
LKO
α-FLAG IPs
Ub-proteins
input
F
ddFKBP12-AP
DMSO
Shield1
Chase (h): 0 1 2 4 0 1 2 4
100
75
50
25
0
% of total
Shield1
DMSO
0
1
2
4
Time (h)

Figure 5. Protein folding status determines nascent chain re-ubiquitination and degradation.

(A) 293T cells expressing the indicated HA-tagged constructs were subjected to anti-HA magnetic beads and analyzed by immunoblotting for the indicated antigens.

(B) FLAG-XBP1u or its mutant were transfected along with HA-ubiquitin into cells treated with either control siRNA or RNF126 siRNA. Cell lysates were IPed with anti-FLAG beads and probed for Ub-proteins using an HA antibody and for XBP1u with an anti-FLAG antibody.

(C) CHX chase analysis was performed in cells treated with indicated siRNA and expressing XBP1u or XBP1u-AP*, followed by immunoblotting for the indicated antigens.

(D) (Top) Model construct illustrating the destabilized domain (dd) comprising FKBP12 fused with the arrest peptide (AP) of XBP1u. (Bottom) Schematic representation of LTN1-mediated ubiquitination of ddFKBP12-AP nascent chain. Shield1 small molecule is known to stabilize the folding of ddFKBP12.

(E) WT or LTN1 KO cells expressing dd FKBP12-AP alongside HA-ubiquitin were untreated or treated with Shield1, immunoprecipitated, and analyzed by immunoblotting.

(F) Pulse-chase experiments were conducted using cells expressing ddFKBP12-AP, treated either with or without Shield1.

See also **Figure S5**

Figure 6

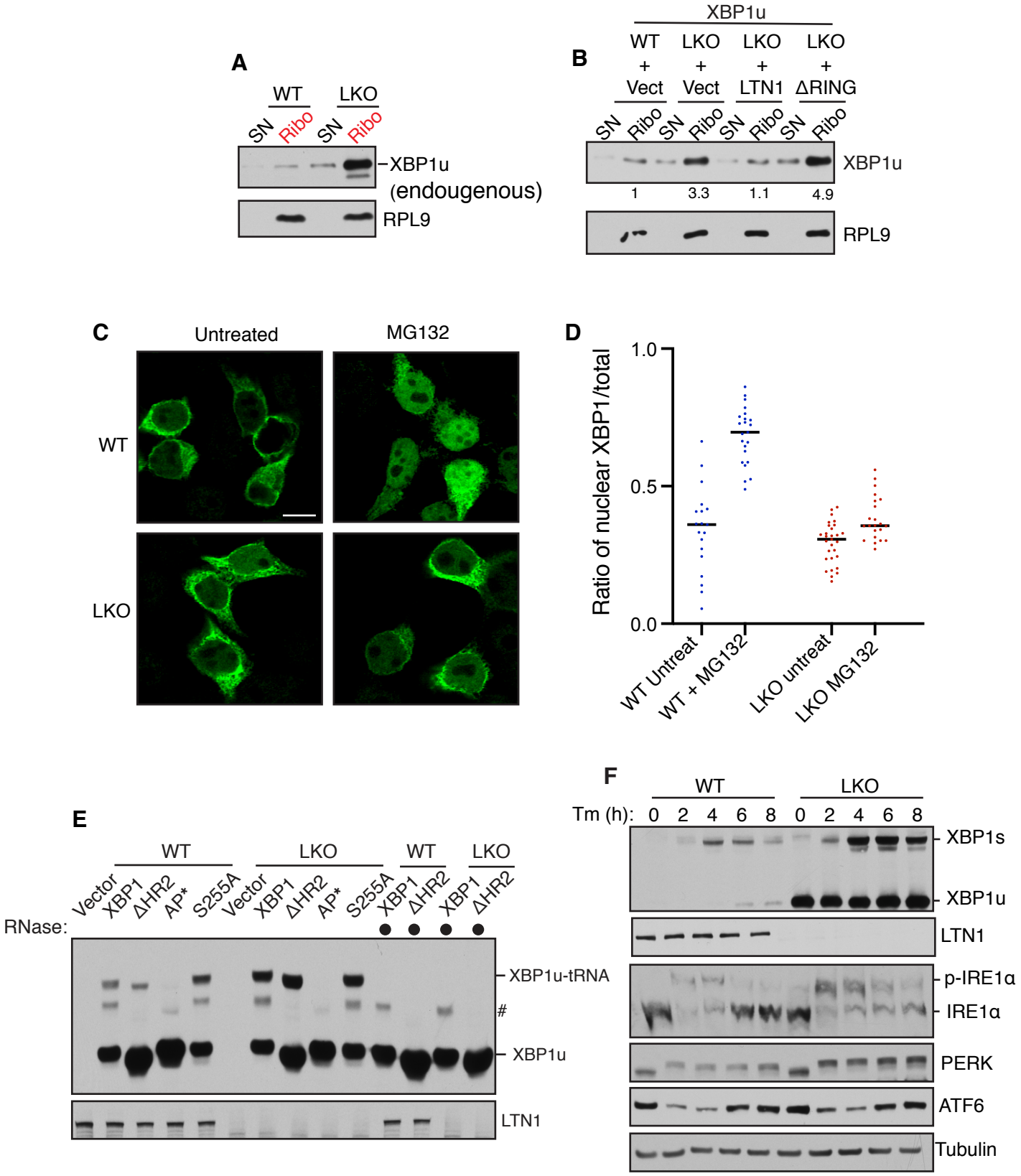
A
WT
LKO
SN
Ribo
SN
Ribo
XBP1u
(endougenous)
RPL9
B
XBP1u
WT + Vect
LKO + Vect
LKO + LTN1
LKO + ΔRING
SN
Ribo
SN
Ribo
SN
Ribo
SN
Ribo
XBP1u
1
3.3
1.1
4.9
RPL9
C
Untreated
MG132
WT
LKO
D
Ratio of nuclear XBP1/total
1.0
0.5
0.0
WT Untreat
WT + MG132
LKO untreat
LKO MG132
E
WT
LKO
WT
LKO
Vector
XBP1
ΔHR2
AP*
S255A
Vector
XBP1
ΔHR2
AP*
S255A
XBP1
ΔHR2
XBP1
ΔHR2
RNase:
XBP1u-tRNA
#
XBP1u
LTN1
F
WT
LKO
Tm (h): 0 2 4 6 8 0 2 4 6 8
XBP1s
XBP1u
LTN1
p-IRE1α
IRE1α
PERK
ATF6
Tubulin

Figure 6. The unfolded protein response (UPR) is dysregulated in LTN1-depleted cells.

(A) Immunoblotting analysis of endogenous XBP1u in supernatants and ribosome fractions from WT or LKO cells.

(B) Cells expressing indicated plasmids were fractionated into supernatents and ribosomes and analyzed by immunoblotting for the indicated antigens.

(C) WT or LKO cells expressing XBP1u were either untreated or treated with 20μM MG132 for 30min. Subsequently, cells were processed using an immunostaining procedure to label XBP1u (green) with rat anti-FLAG. Scale bars are 10 μm.

(D) Quantification of (C) from at least two independent experiments (means ± SEM).

(E) Cell lysates expressing the indicated variants of XBP1u were separated under neutral pH conditions (NuPAGE) to preserve peptidyl-tRNA ester bonds. Note that tRNA-linked XBP1u was sensitive to RNase treatment.

(E) WT or LKO cells were treated with tunicamycin (Tm: 5μg/ml) and analyzed for immunoblotting for the indicated antigen. Note that the loss of signal represents the activation of ATF6 during ER stress.

See also **Figure S6**

Figure 7

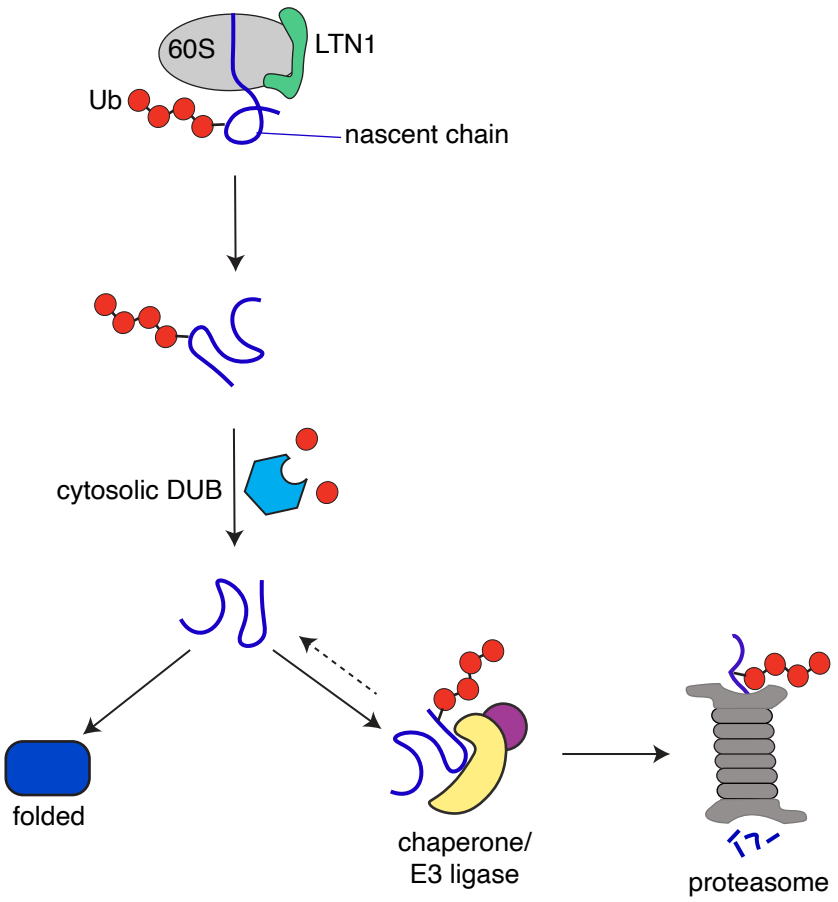

Figure 7: A model for triaging ubiquitinated nascent proteins between maturation and degradation. Upon release from stalled ribosomes, nascent proteins polyubiquitinated by the LTN1 E3 ligase are promptly deubiquitinated in the cytosol. This decoupling from immediate proteasomal degradation provides a secondary chance for some nascent proteins to achieve proper folding and maturation. However, if a nascent protein fails to attain stability and exposes a degron, it undergoes re-ubiquitination through cytosolic quality control mechanisms, leading to proteasomal degradation. It is conceivable that the nascent protein may re-enter a similar cycle, but ultimately, it would face degradation by the proteasome if it remains exposed to a degron for an extended period.